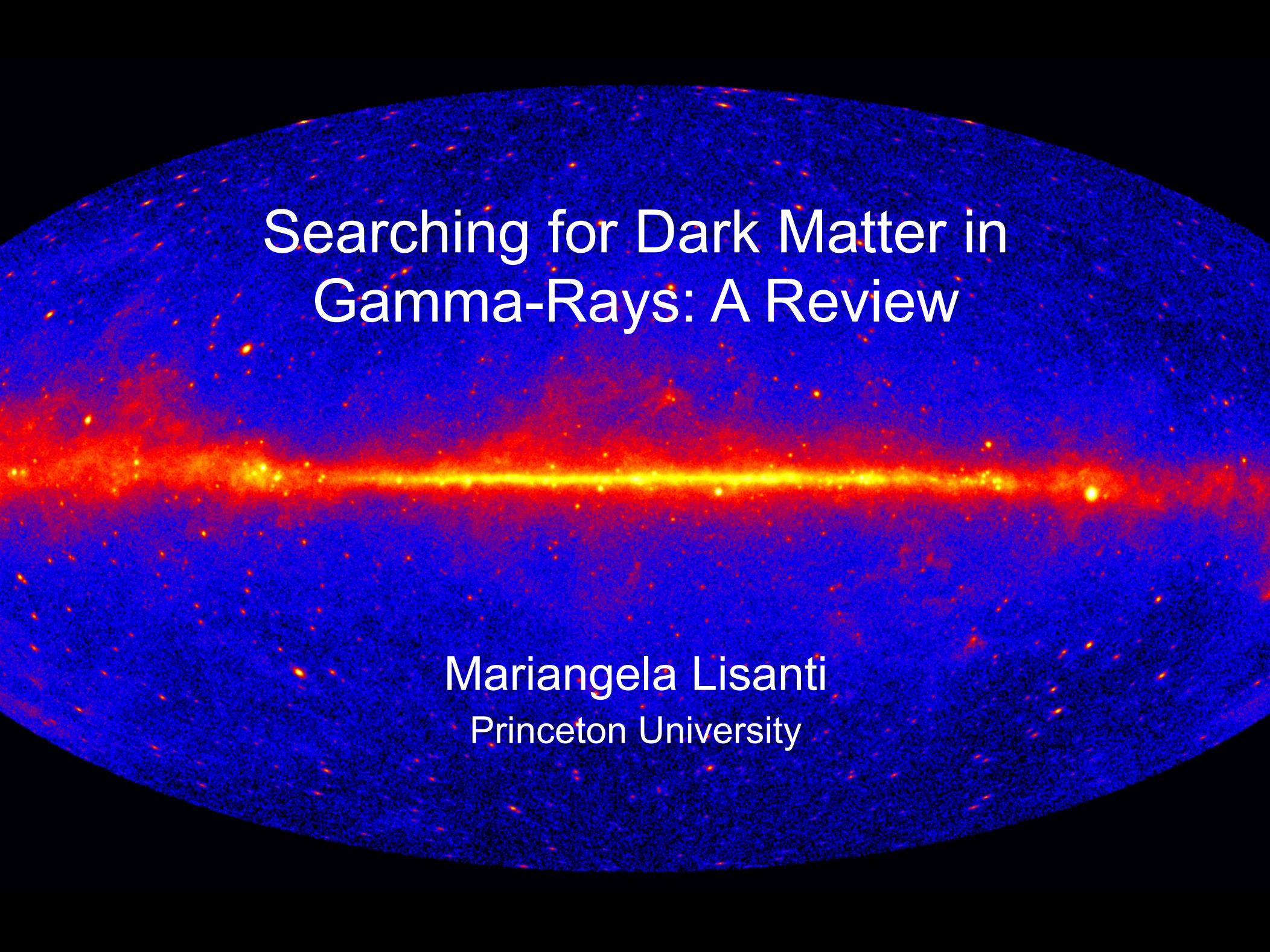

# Searching for Dark Matter in Gamma-Rays: A Review

Mariangela Lisanti
Princeton University

# Touring the Gamma-Ray Sky

^ Fermi

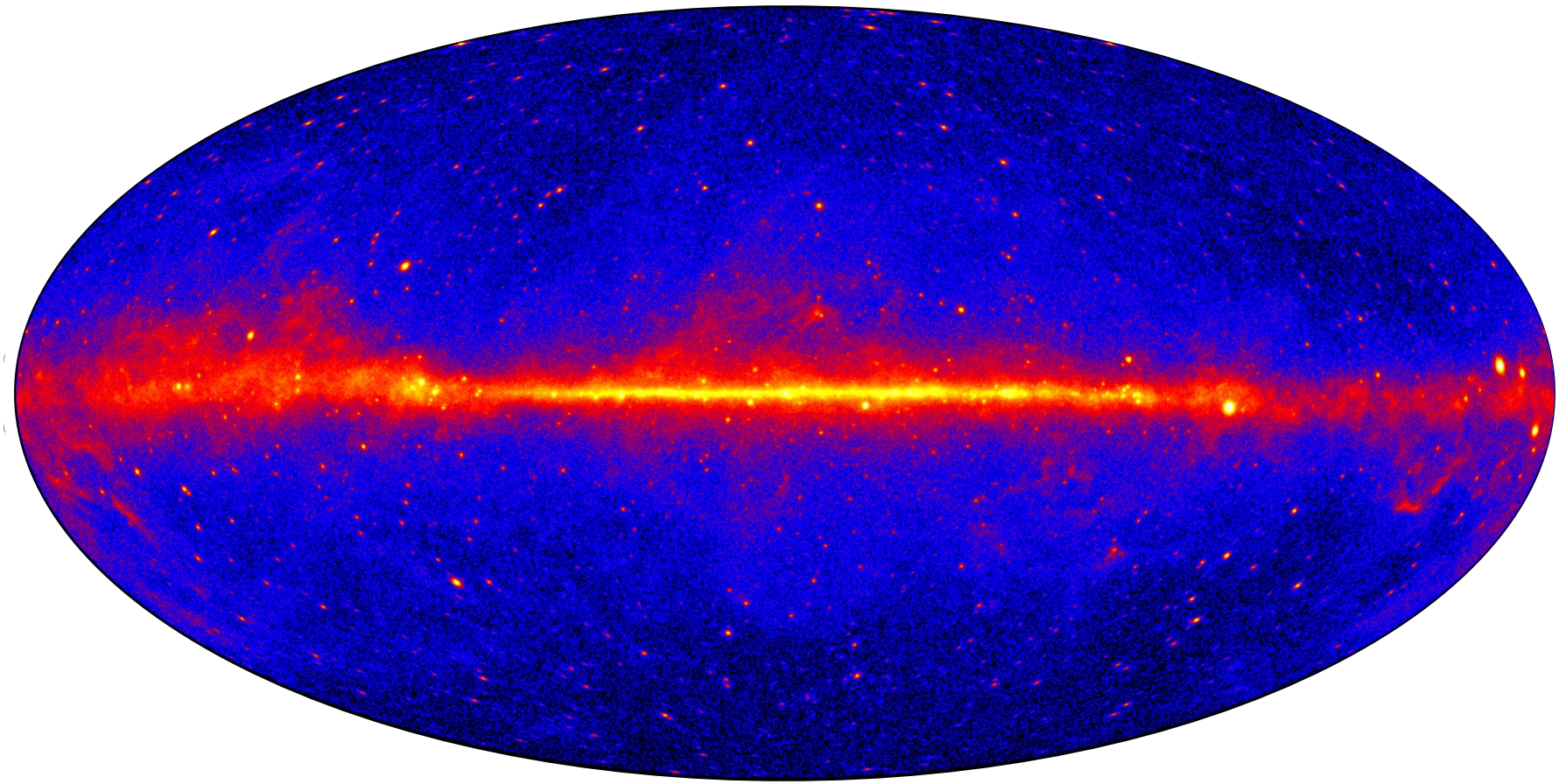

# Diffuse Gamma Rays

High-energy $\gamma$-rays produced through propagation of cosmic rays in the Galaxy

## Bremsstrahlung

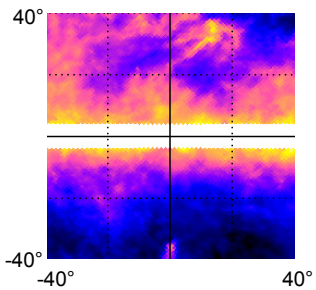


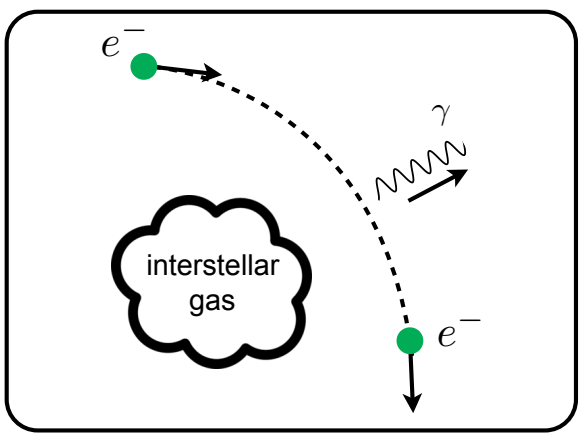


## Pion Emission

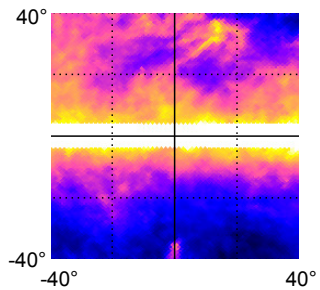


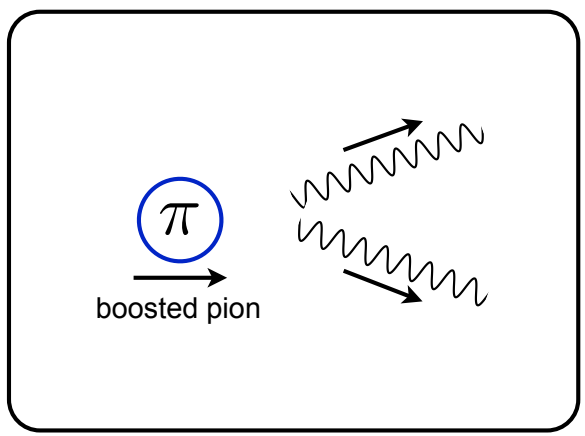


## Inverse Compton

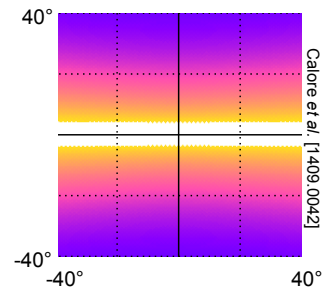


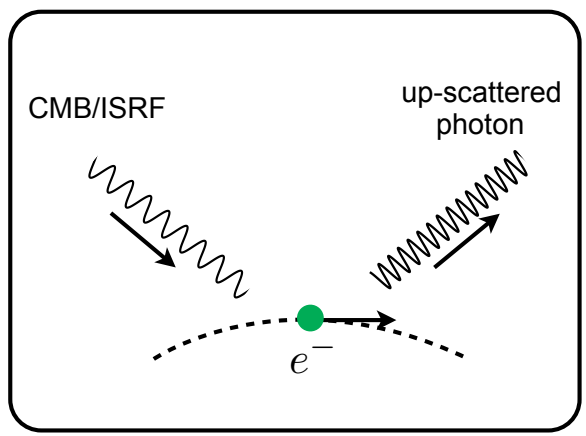

# Touring the Gamma-Ray Sky

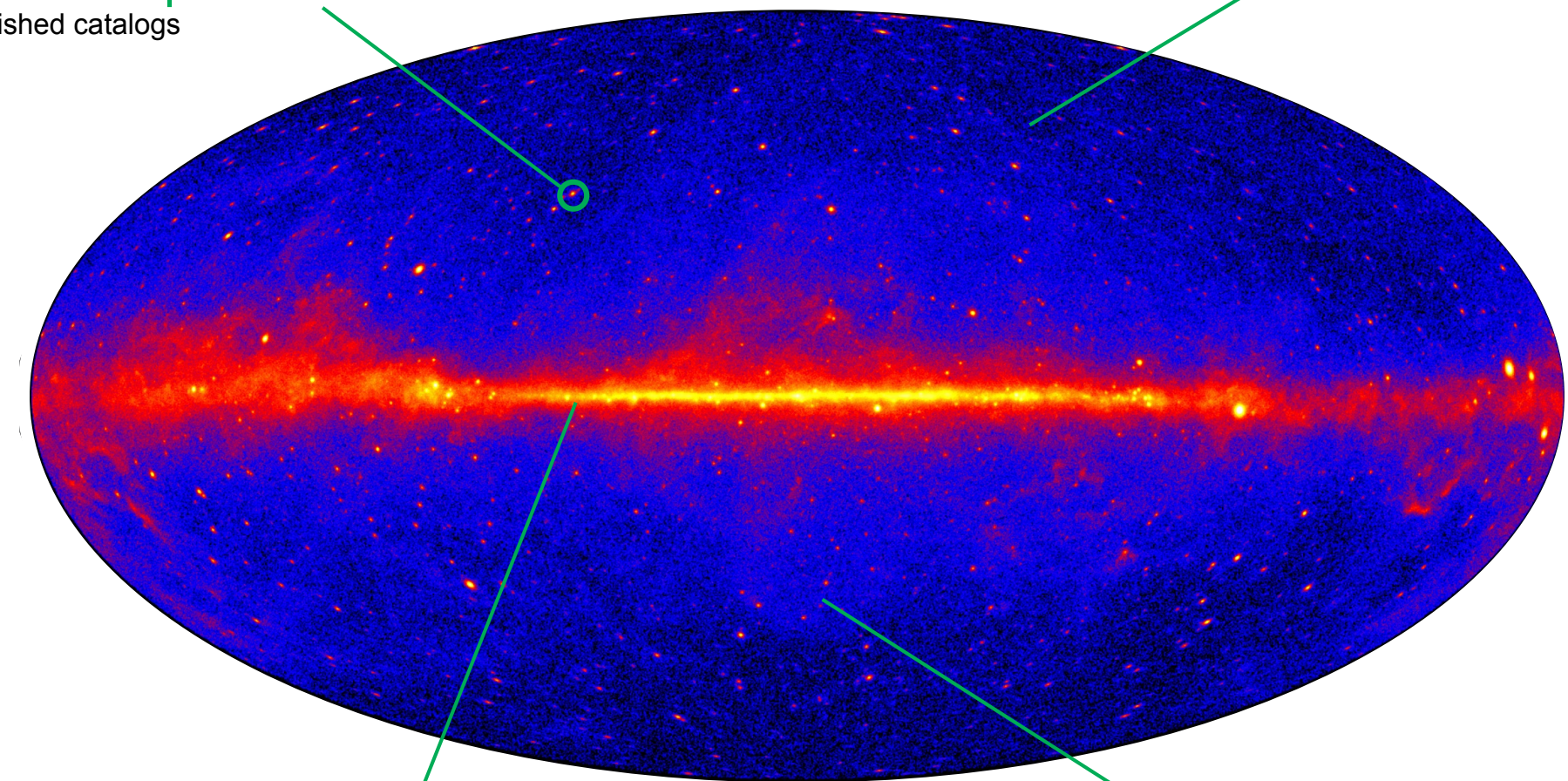

# The Templates

Each component contributing to the gamma-ray emission is modeled as a ‘template’

The fitting procedure determines how much flux is attributed to each template

Galactic Diffuse Emission

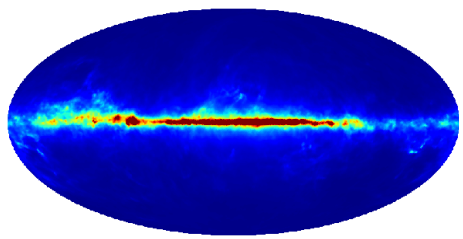

Fermi Bubbles

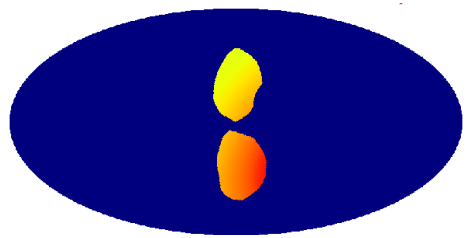

Extragalactic (Isotropic)

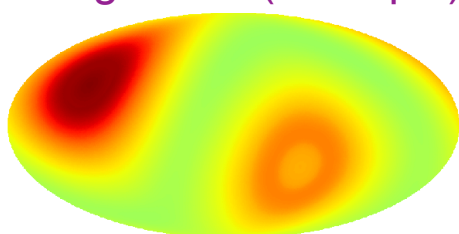

Dark Matter (NFW)

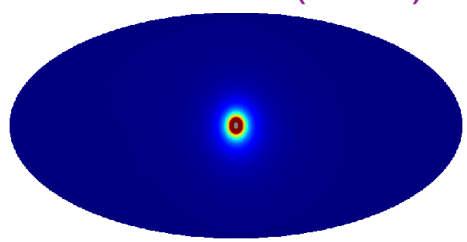

Inherent uncertainties due to assumptions about the spatial distributions (as well as number) of templates that are included in the analysis

# Where to Look for Dark Matter

The photon flux for dark matter annihilation is given by

$$\Phi(E,\psi) = \overbrace{\frac{\sigma_{\rm A} v}{8\pi m_\chi^2}\frac{dN_\gamma}{dE}}^{\text{particle physics}} \overbrace{\int d\ell\, \rho\left[r(\ell,\psi)\right]^2}^{\text{J-factor}}$$

J-factor depends on the dark matter density profile

$$\rho_{\rm NFW}(r) \propto \frac{(r/r_s)^{-\gamma}}{(1+r/r_s)^{3-\gamma}}$$

Best to look for dark matter annihilation at centers of galaxies, where density is highest

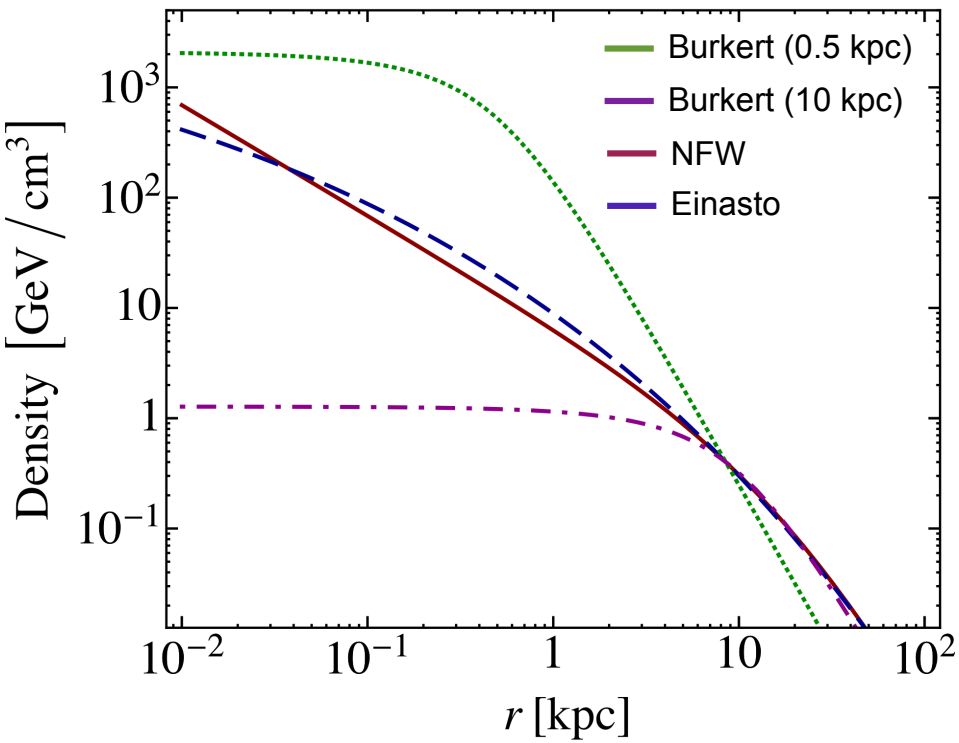

# The Galactic Center

# GeV Photon Excess

Spherically symmetric gamma-ray excess in the Inner Galaxy

Extends out 10˚ (~5000 lyr) from the center of Galaxy

Constitutes ~10% total flux

High statistical significance

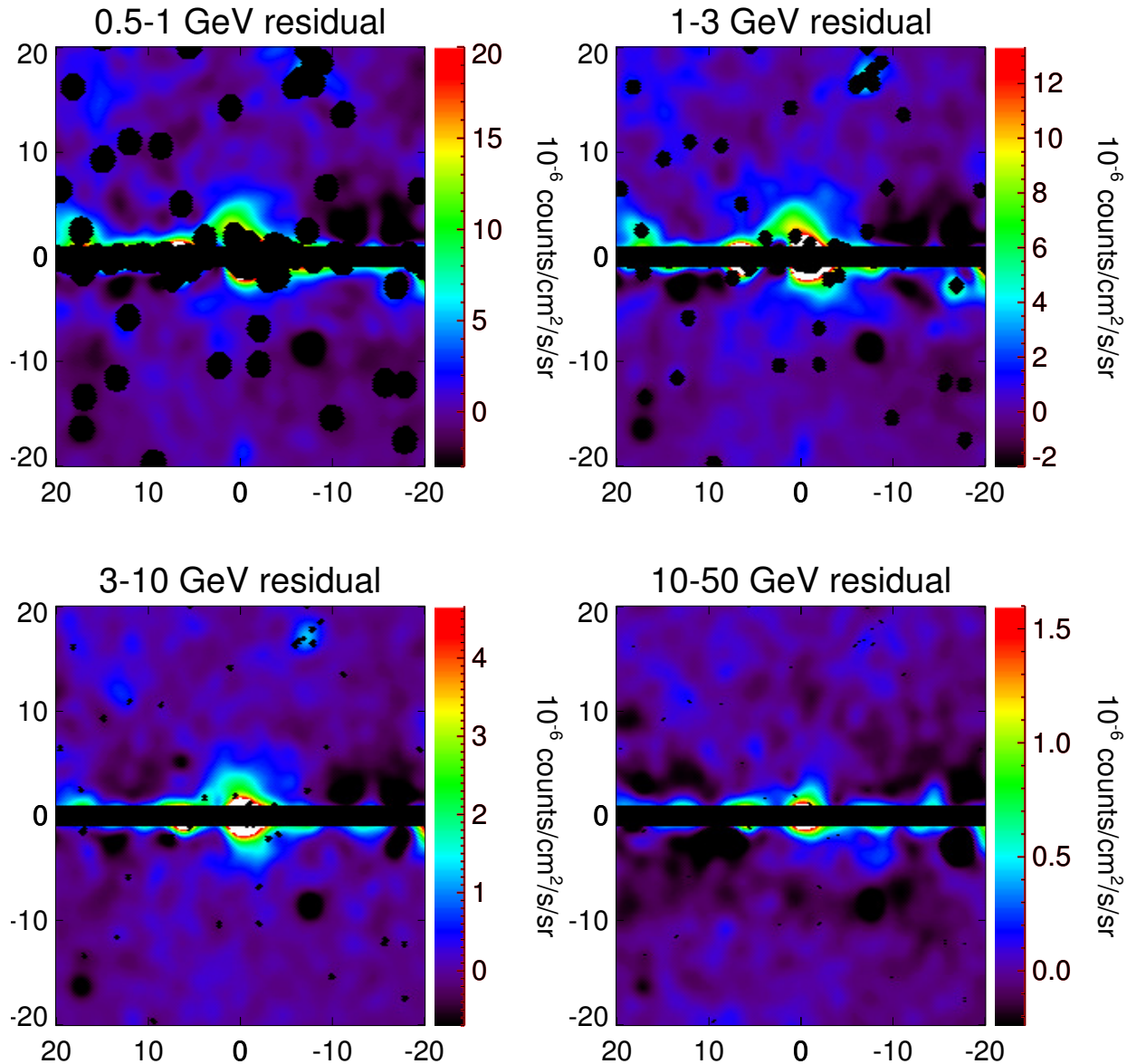


Daylan, Finkbeiner, Hooper, Linden, Portillo, Rodd, and Slatyer [1402.6703]

Goodenough and Hooper [0910.2998]
Hooper and Goodenough [1010.2752]
Boyarsky, Malyshev, Ruchayskiy [1012.5839]
Hooper and Linden [1110.0006]
Abazajian and Kaplinghat [1207.6047]
Gordon and Macias [1306.5725]
Abazajian *et al.* [1402.4090]
Daylan *et al.* [1402.6703]
Calore, Cholis, and Weniger [1409.0042]
*Fermi* Collaboration [1511.02938, 1704.03910]

# GeV Photon Excess

Spatial morphology and energy spectrum of excess is consistent with dark matter expectation

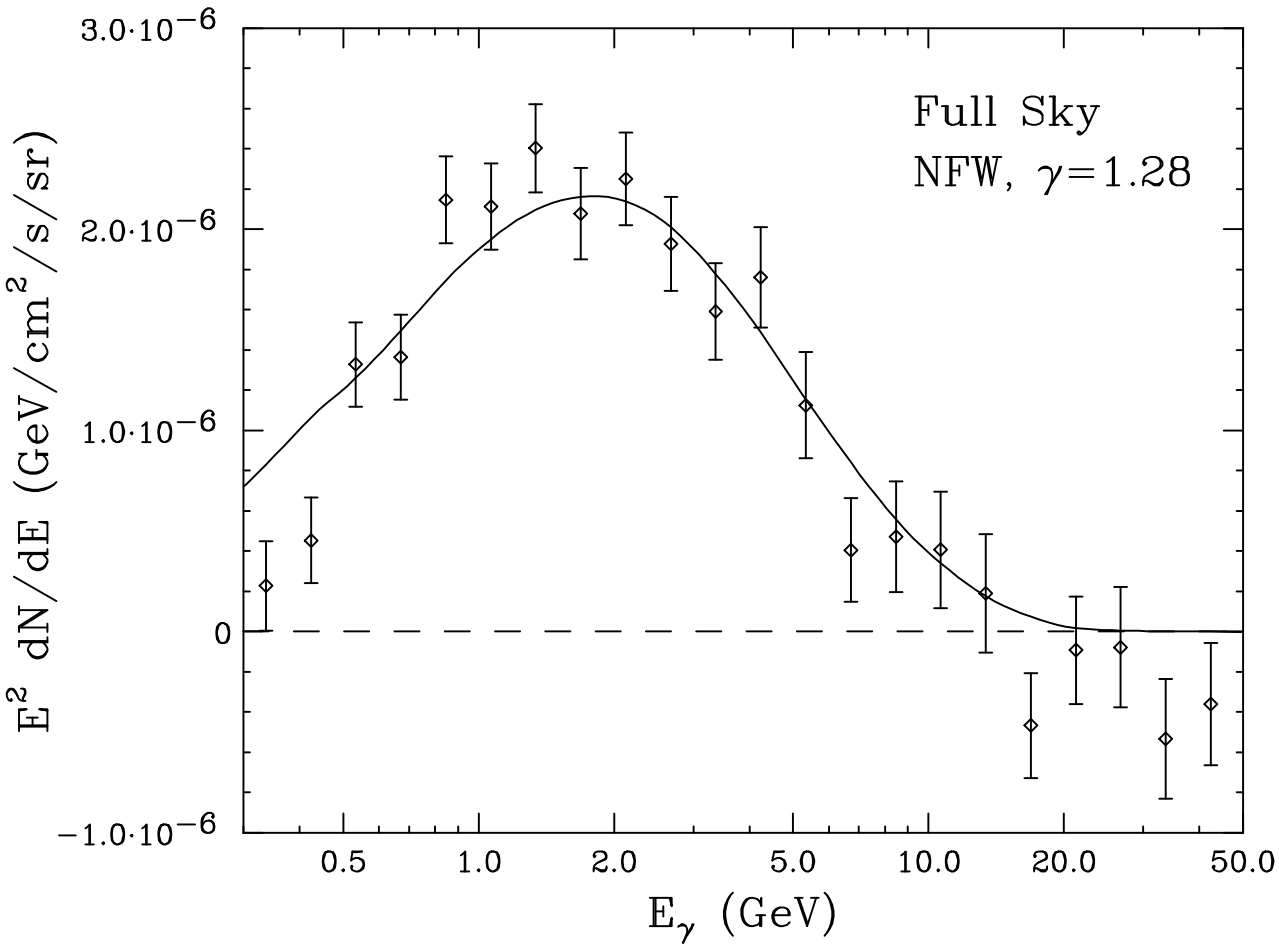


Daylan *et al.* [1402.6703]

# GeV Photon Excess

Spatial morphology and energy spectrum of excess is consistent with dark matter expectation

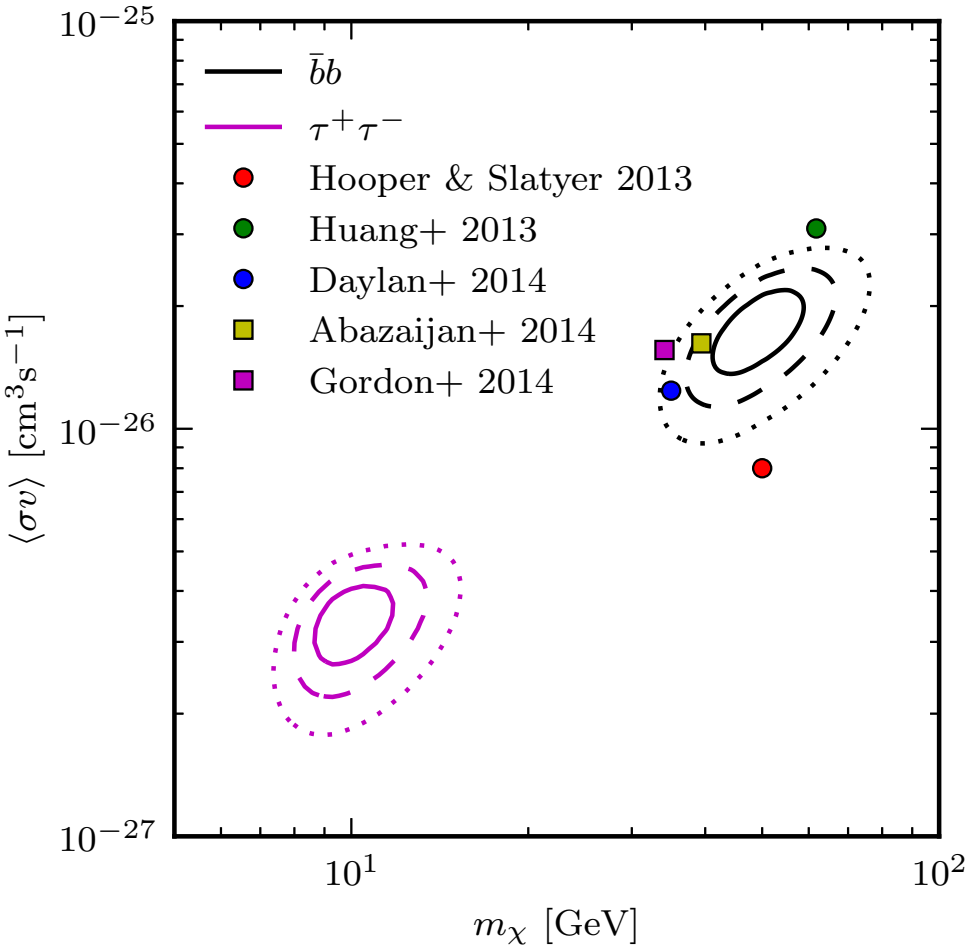


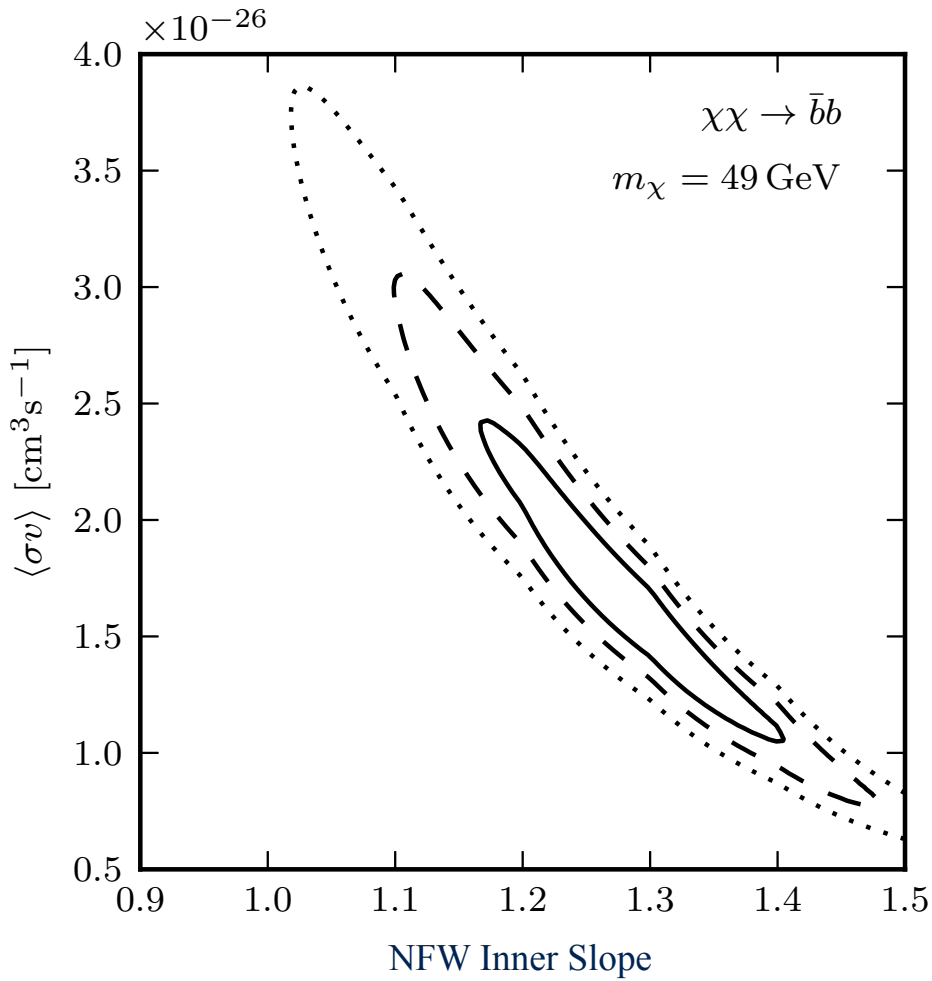


Calore, Cholis, & Weniger [1409.0042]

# Diffuse Foreground Uncertainty

Evidence for excess emission is robust to variations in the models of Galactic diffuse emission, at least within Galprop framework

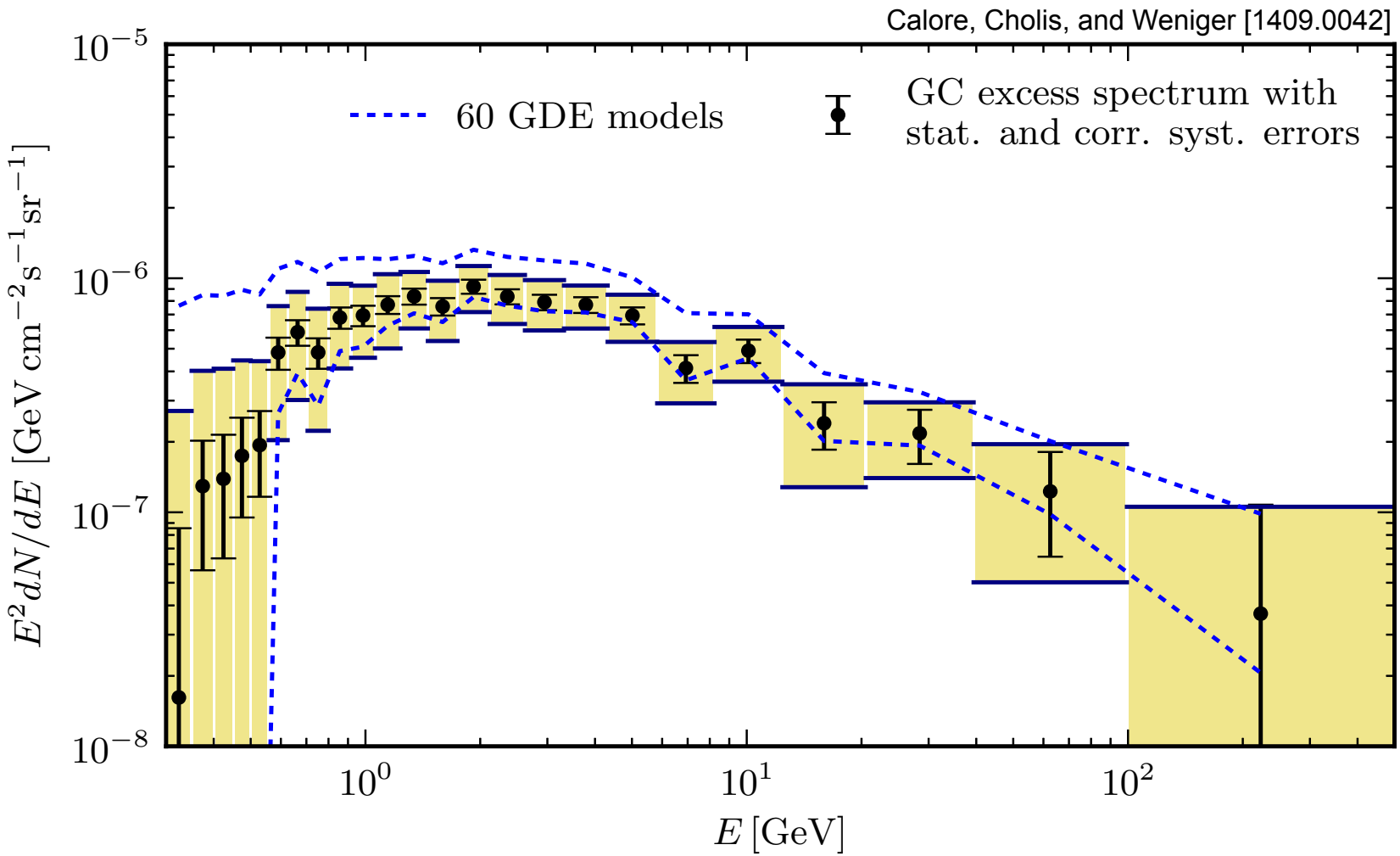

# Unresolved Sources

GeV Excess could also be explained by a population of unresolved sources just below *Fermi*'s detection threshold

Rapidly-spinning neutron stars, called millisecond pulsars, are potential candidates

Abazajian [1011.4275]

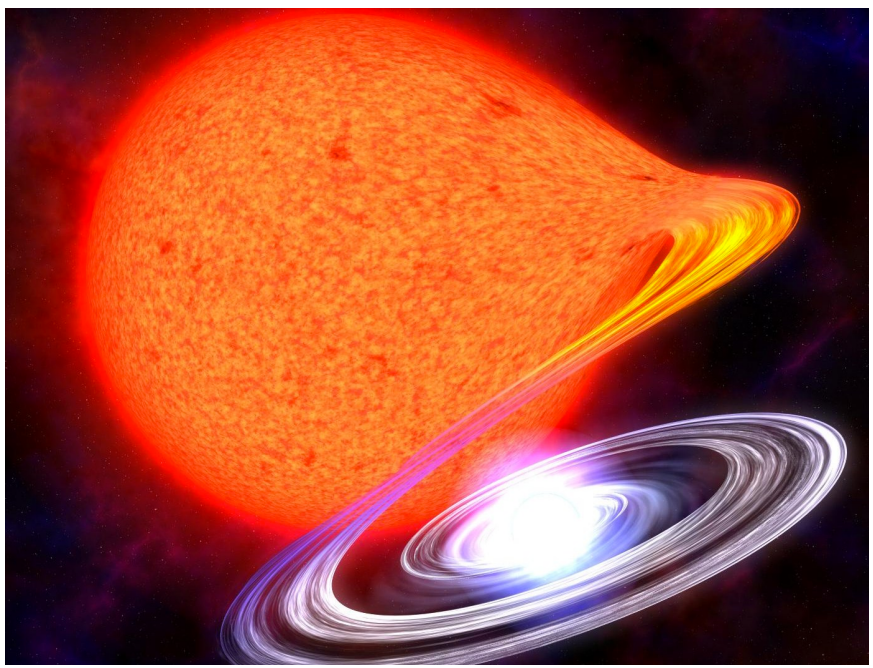

https://apatruno.files.wordpress.com/2013/09/binarystarcataclysm.jpg

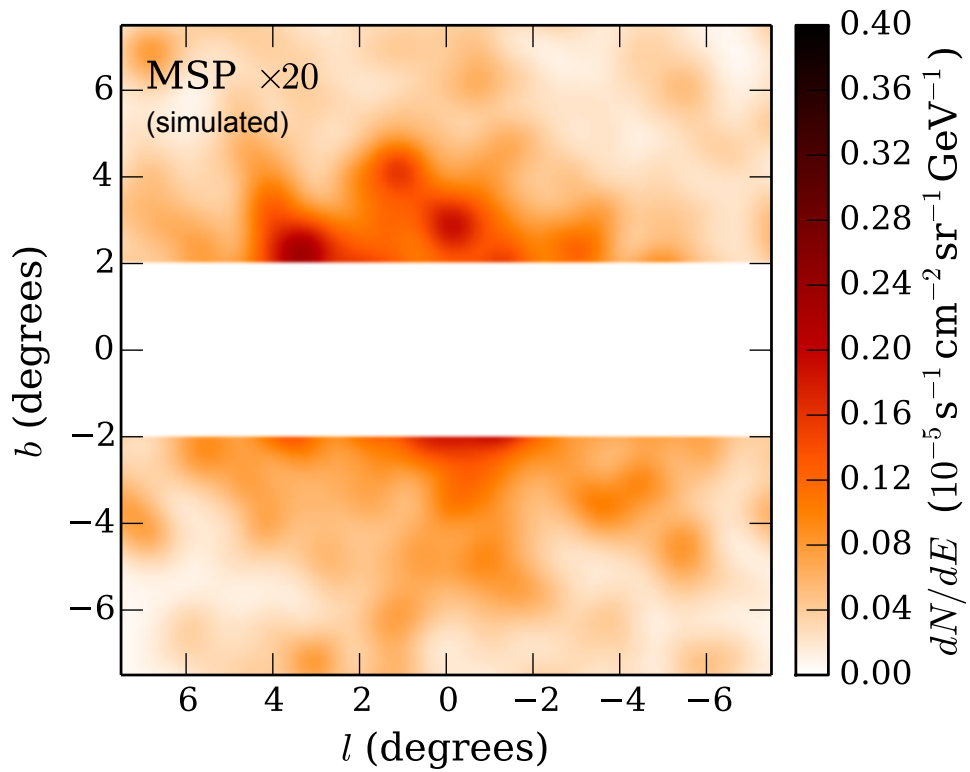


O'Leary *et al.* [1601.05797]

# Photon Statistics

Apply image processing techniques to distinguish dark matter from unresolved astrophysical sources

Malyshev and Hogg [1104.0010]; Lee, Lisanti, and Safdi [1412.6099]

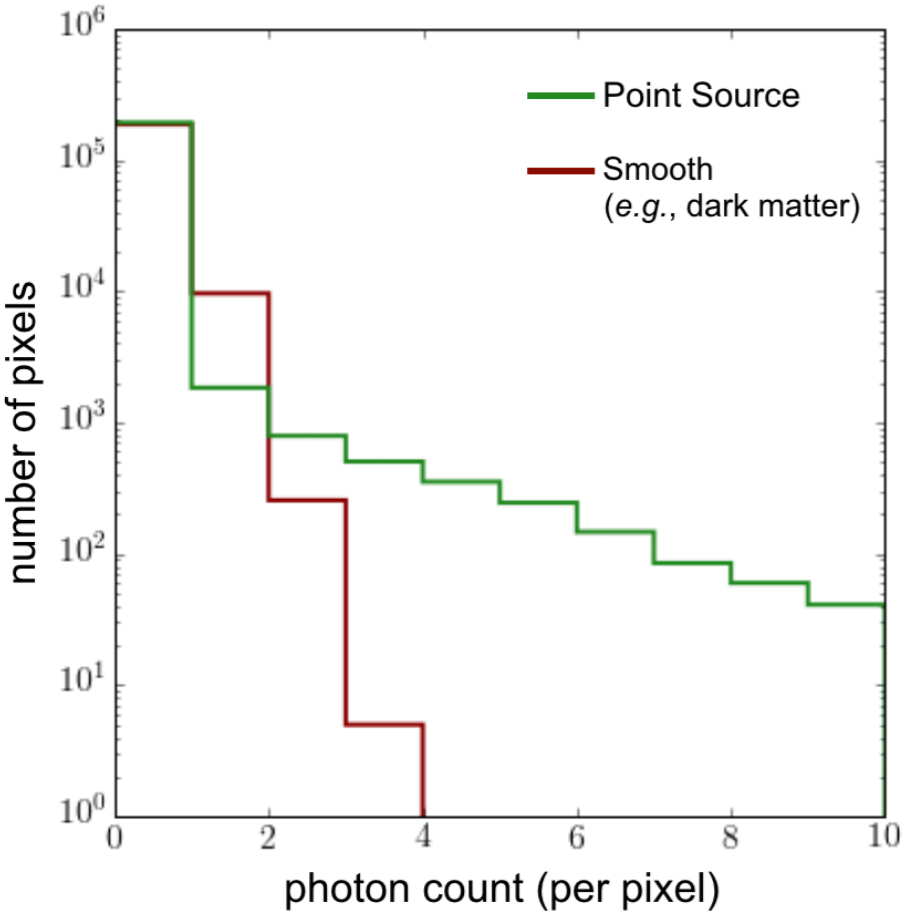


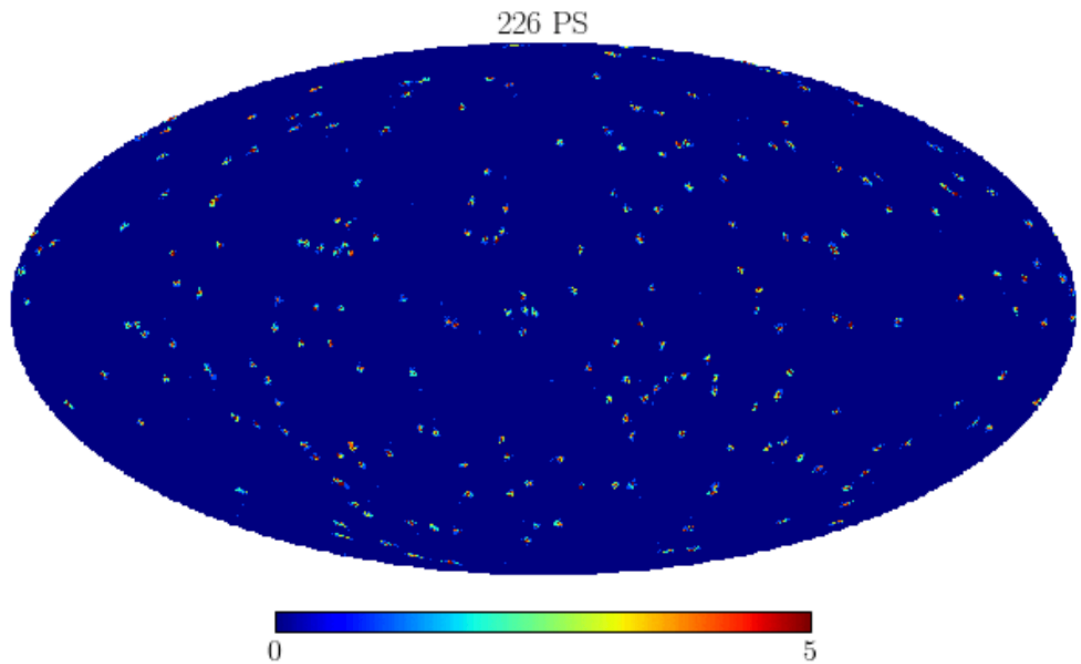

# Photon Statistics

Apply image processing techniques to distinguish dark matter from unresolved astrophysical sources

Malyshev and Hogg [1104.0010]; Lee, Lisanti, and Safdi [1412.6099]

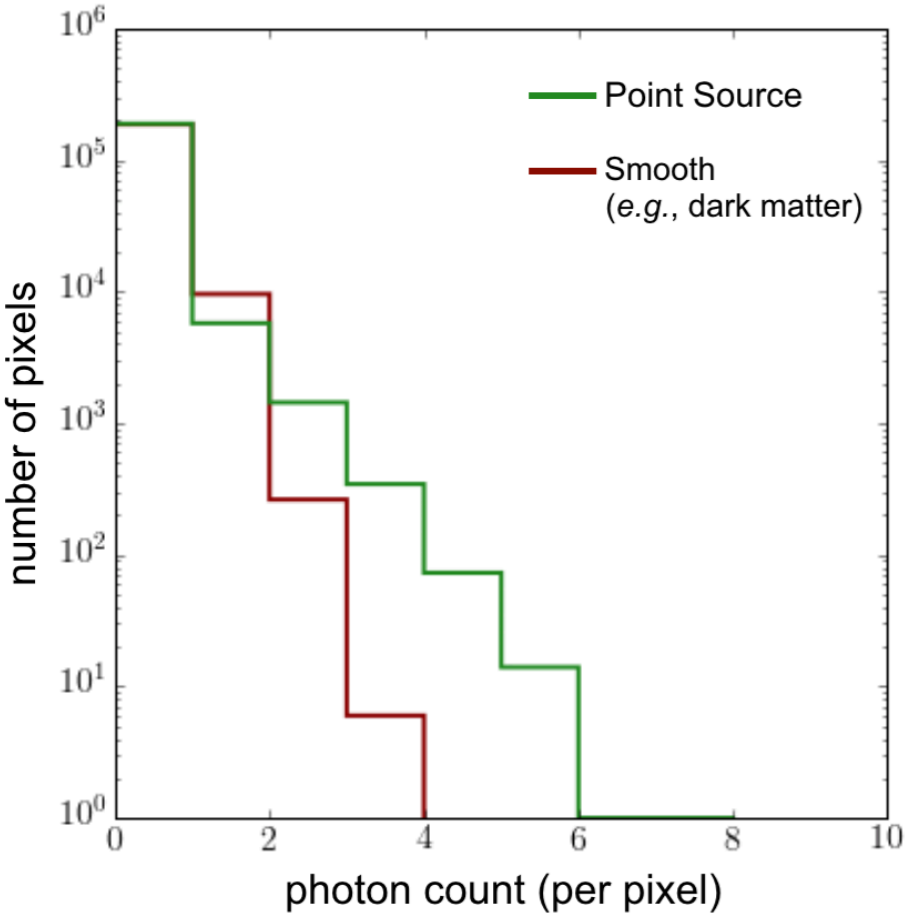


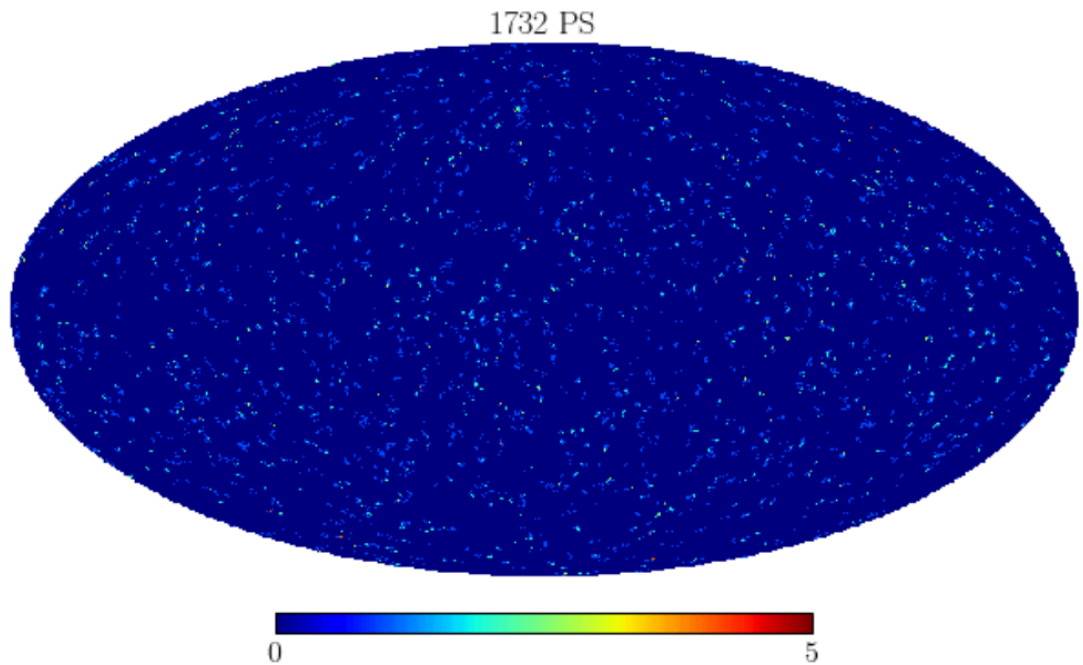

# Inner Galaxy Analysis

Study of photon statistics in the Inner Galaxy provides strong evidence for a population of unresolved astrophysical sources

Lee, Lisanti, Safdi, Slatyer, and Xue [1506.05124]

Complimentary study using wavelet methods found similar results

Bartels, Krishnamurthy, and Weniger [1506.05104]

Lee *et al.* (2015)

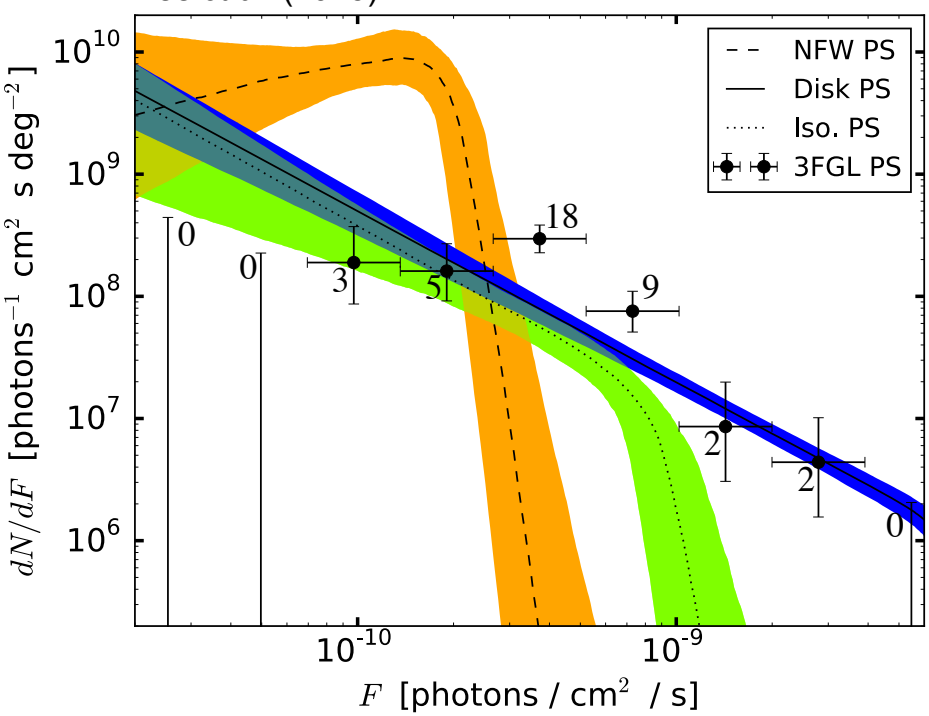


Bartels *et al.* (2015)

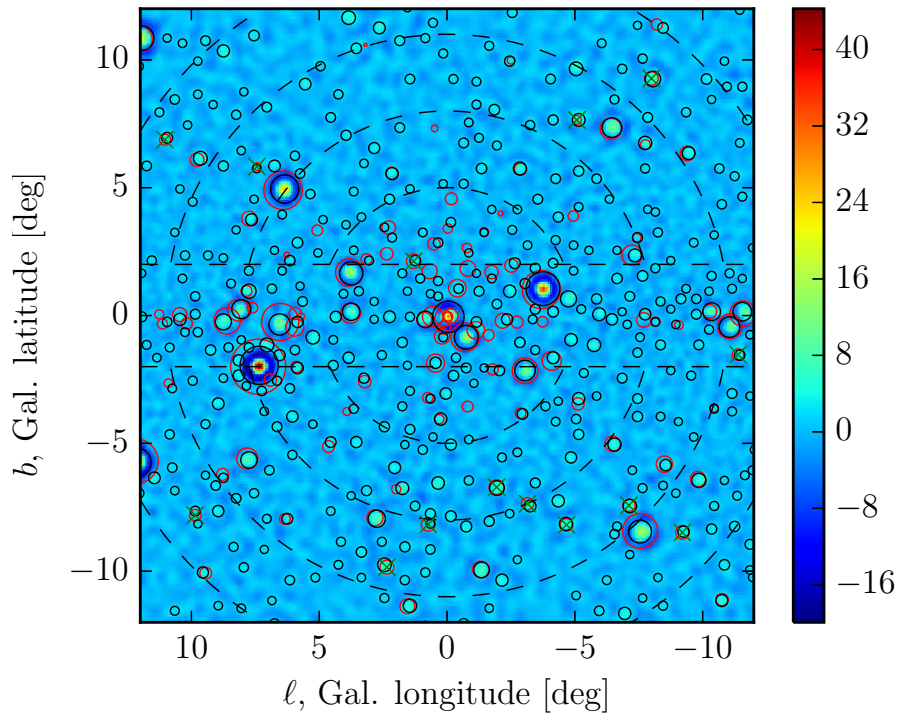

# Stellar Bulge

GeV Excess may better trace the stellar bulge rather than dark matter emission

Macias *et al.* [1507.05616]; Bartels *et al.* [1711.04778]

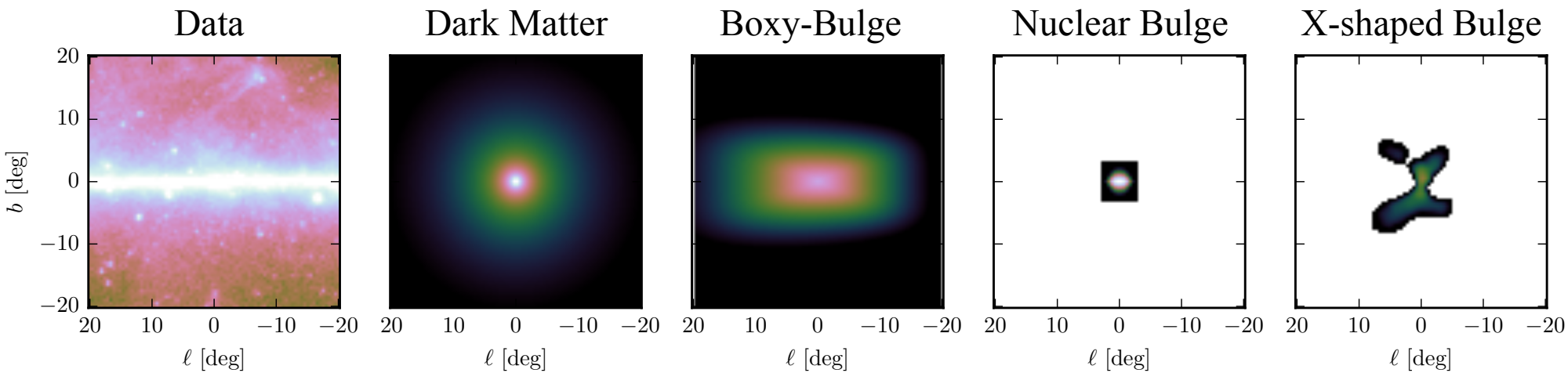


Bartels *et al.* [1711.04778]

This weakens the argument that the morphology of the excess is consistent with dark matter and strengthens the hypothesis that the excess has a stellar origin

# Millisecond Pulsars

MSPs may have been dumped in Inner Galaxy by disrupted globular clusters

Brandt and Kocsis [1507.05616]; see also Hooper and Linden [1606.09250] for summary of challenges

In the coming few years, targeted and large-area radio surveys will be able to detect individual millisecond pulsars if they exist in the Inner Galaxy

Calore *et al.* [1512.06825]

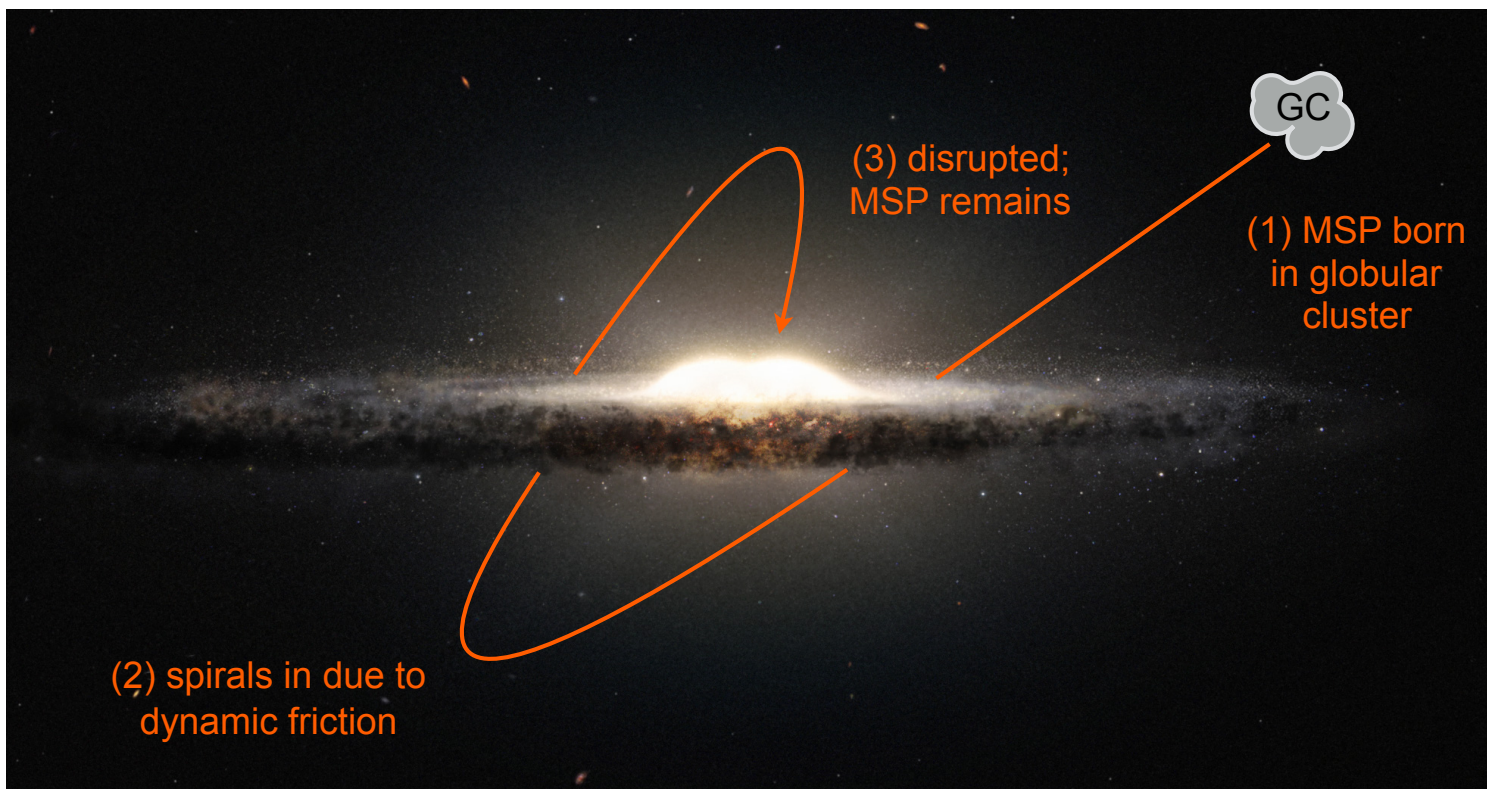


ESO/NASA/JPL-Caltech/M. Kornmesser/R. Hurt

# Einstein@Home MSP

First detection of radio-quiet gamma-ray MSP using Einstein@Home network

Clark *et al.* [1803.06885]

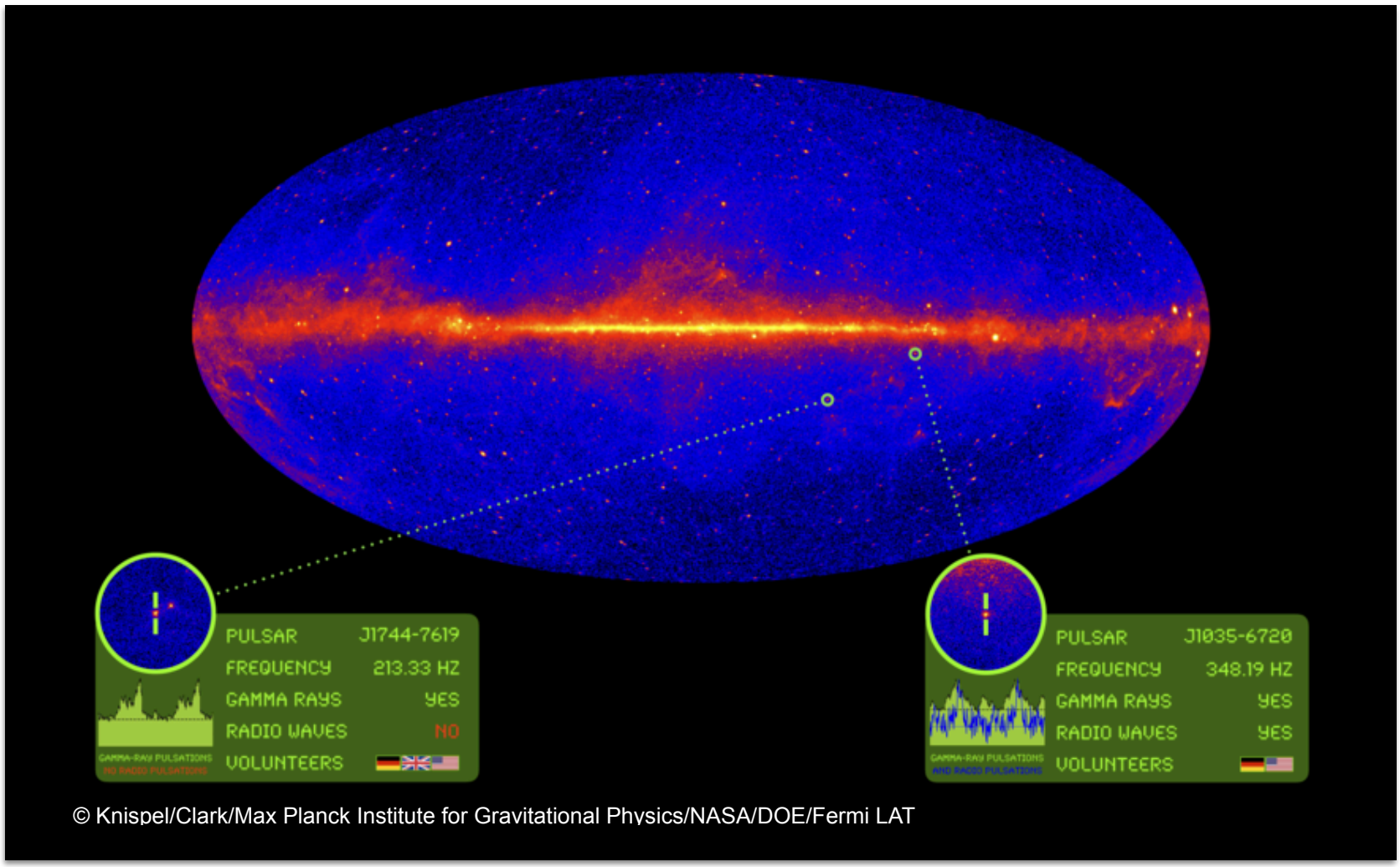

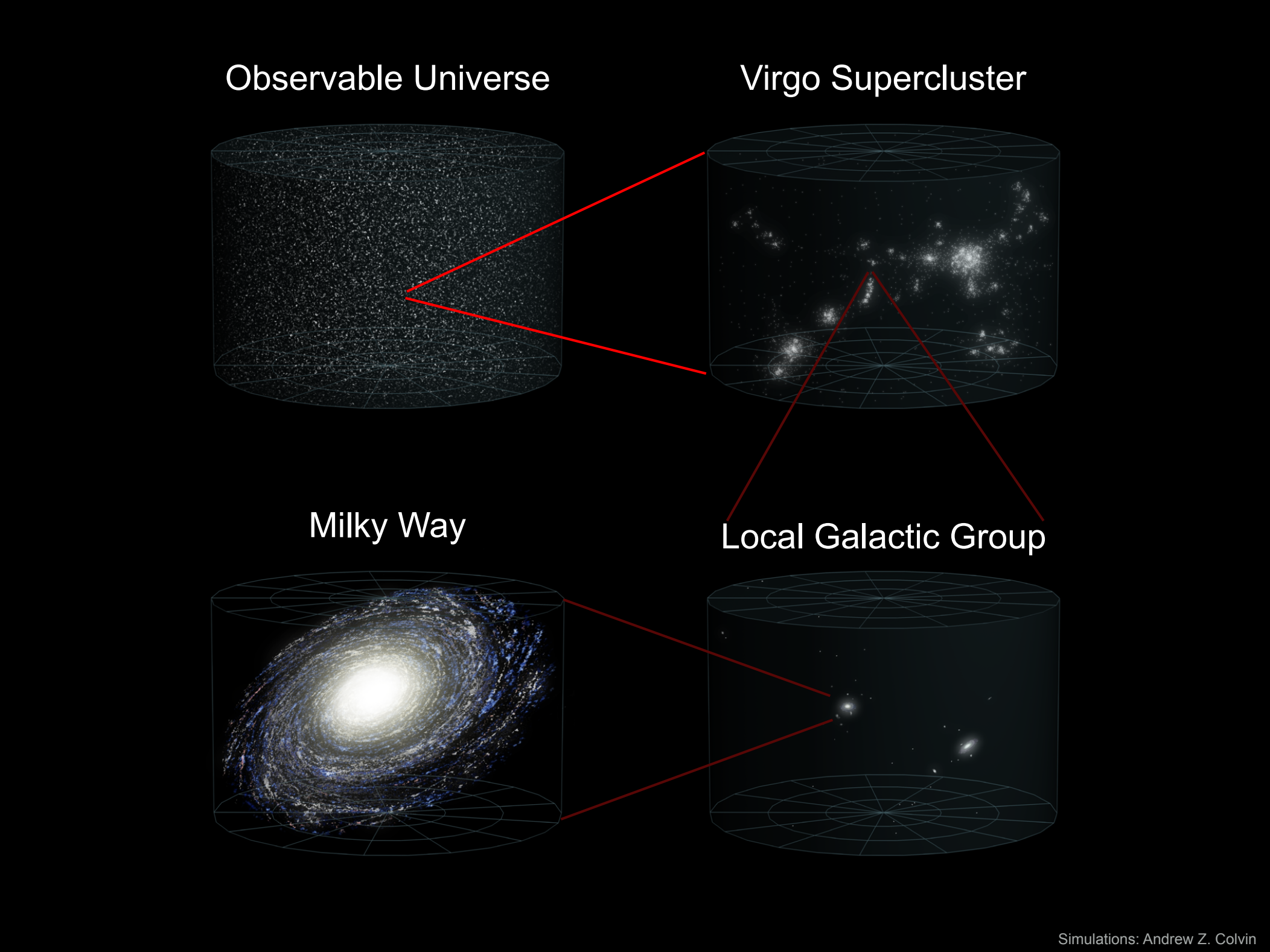
Observable Universe
Virgo Supercluster
Milky Way
Local Galactic Group
Simulations: Andrew Z. Colvin

# Looking Elsewhere

If the GeV Excess is a true dark matter signal, then we should expect to see hints/detections in other astrophysical targets

Dwarf galaxies and galaxy groups are promising options

## Dwarf Galaxies

Relatively ‘clean’ systems; foregrounds better under control

Uncertainties in density distribution: core v. cusp

About 50 known to date

## Galaxy Groups

Cosmic-ray emission from known astrophysical processes

Dark matter signal can be boosted due to substructure—also, difficult to model

In the thousands...

# Dwarf Galaxies

These faint galaxies are dark matter dominated and thus excellent targets for annihilation searches

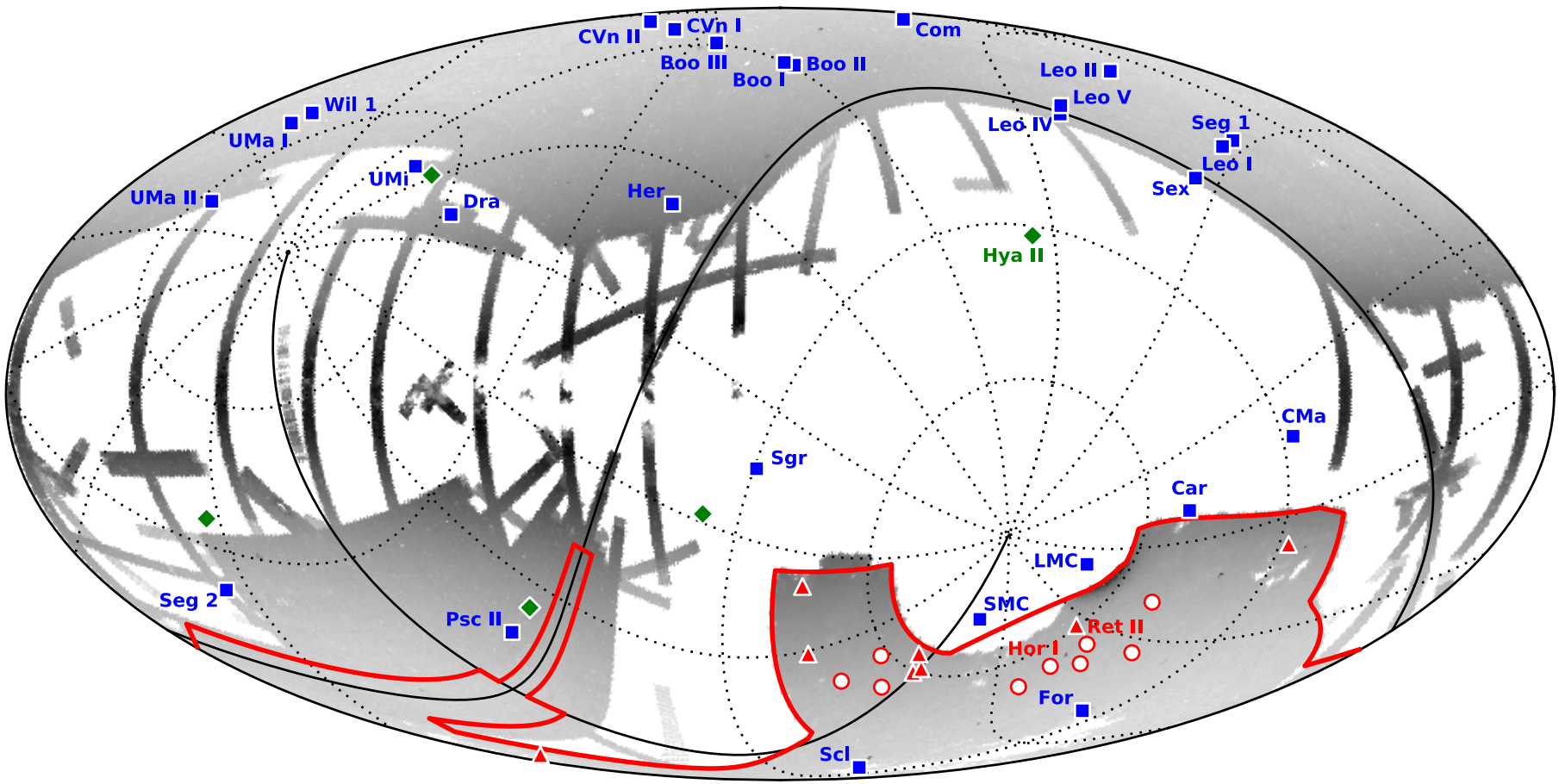


■ Known satellites before 2015

○ ▲ ◆ New Candidates

Drlica-Wagner *et al.* [1508.03622]

# Dwarf Galaxies

Six years of data from *Fermi* LAT used to search for gamma-ray emission from 45 dwarf spheroidal candidates

Observations are becoming sensitive to thermal weak-scale dark matter

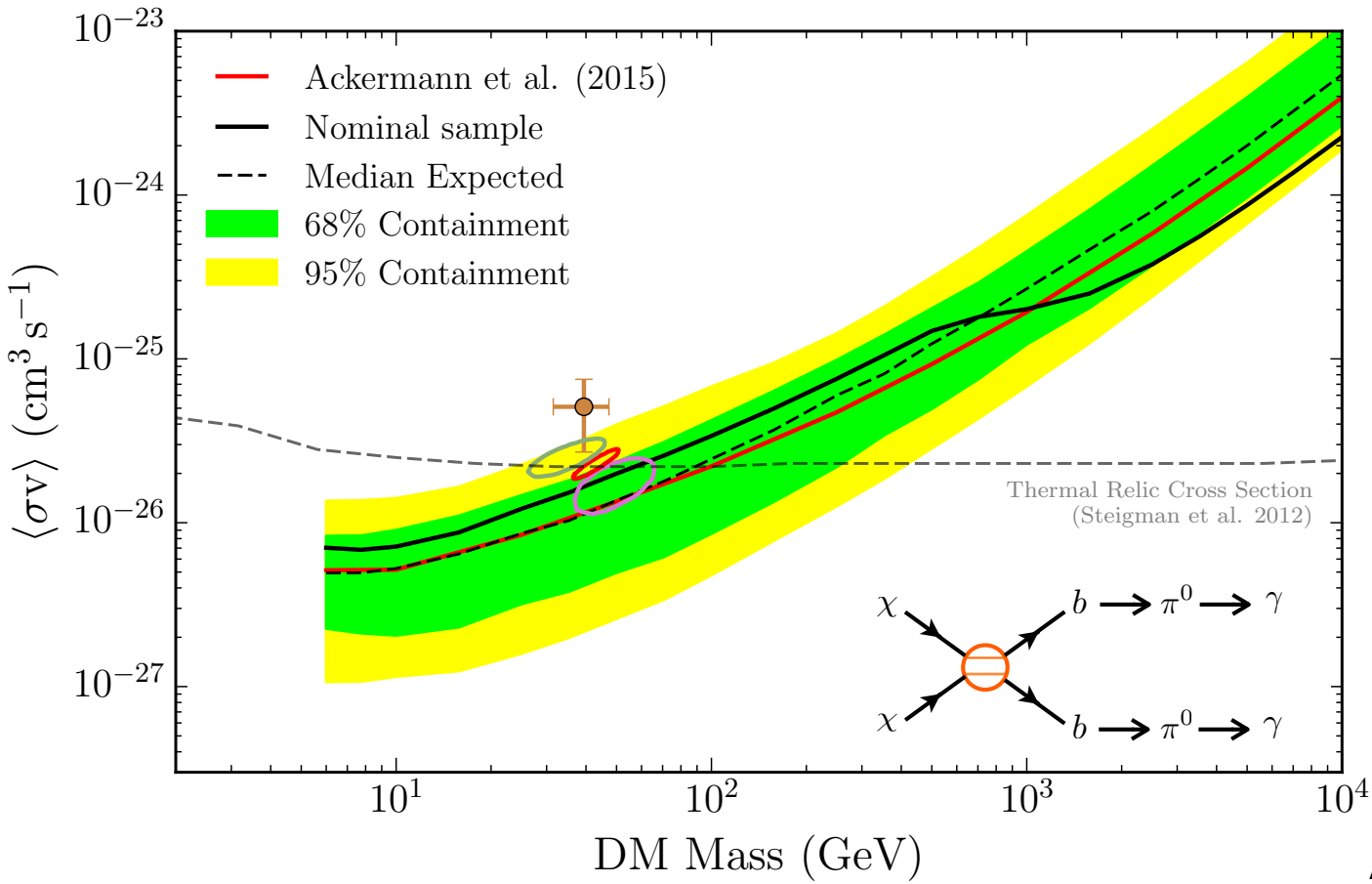


Albert *et al.* [1611.03184]

# From a Group Catalog…

2MASS Redshift Survey is a nearly all-sky near-infrared survey that samples 45,000 galaxies up to redshifts of z~0.03

Bilicki et al. [1311.5246]; Huchra et al. [1108.0669]

Recent catalogs identify groups of nearby galaxies and their associated halo properties

Tully [1503.03134]; Lu et al. [1607.03982]; Kourkchi and Tully [1705.08068]

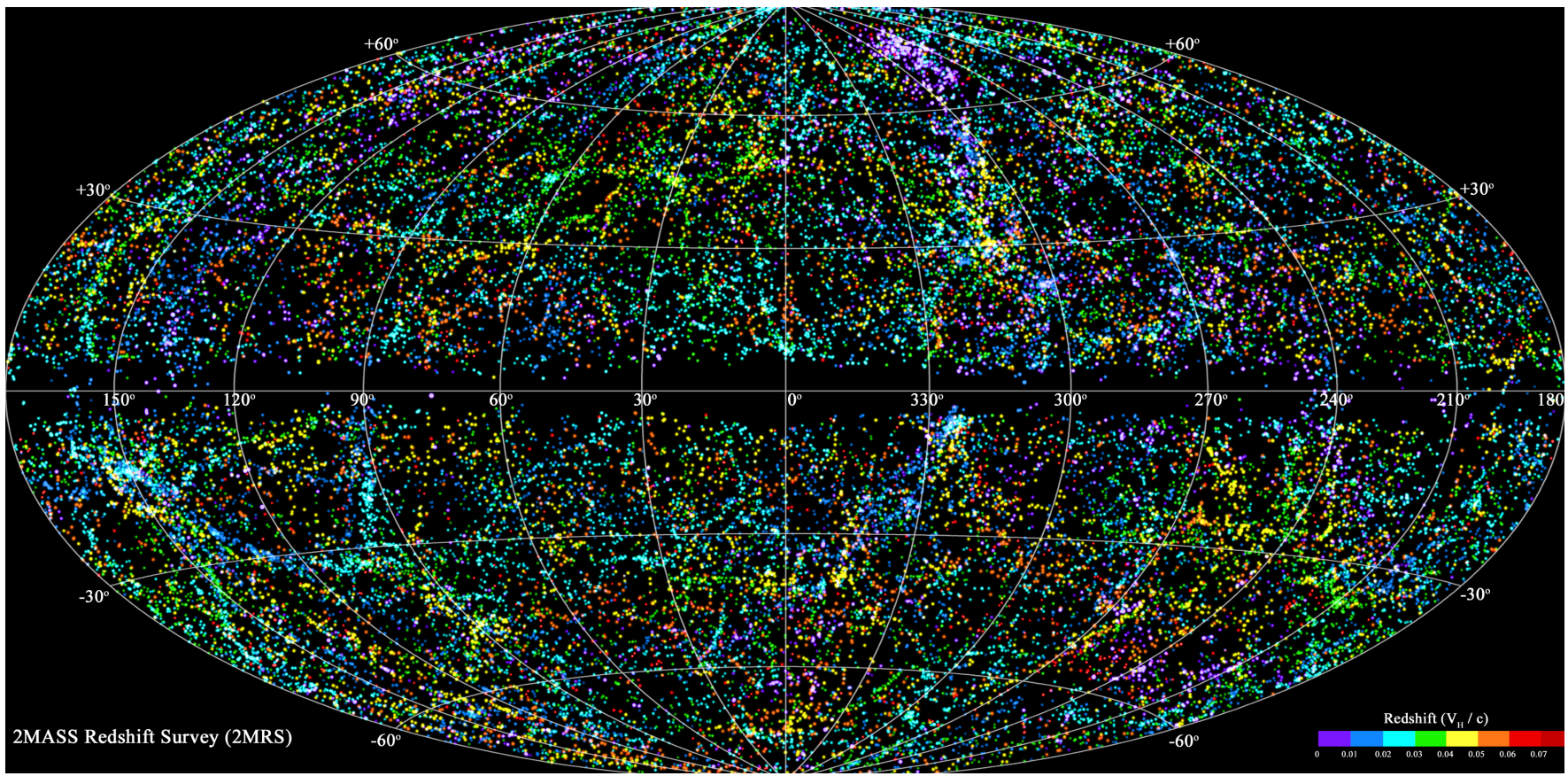

# …to a Dark Matter Sky Map

Lisanti, Mishra-Sharma, Rodd, Safdi, and Wechsler [1709.00416]
Lisanti, Mishra-Sharma, Rodd, and Safdi [1708.09385]

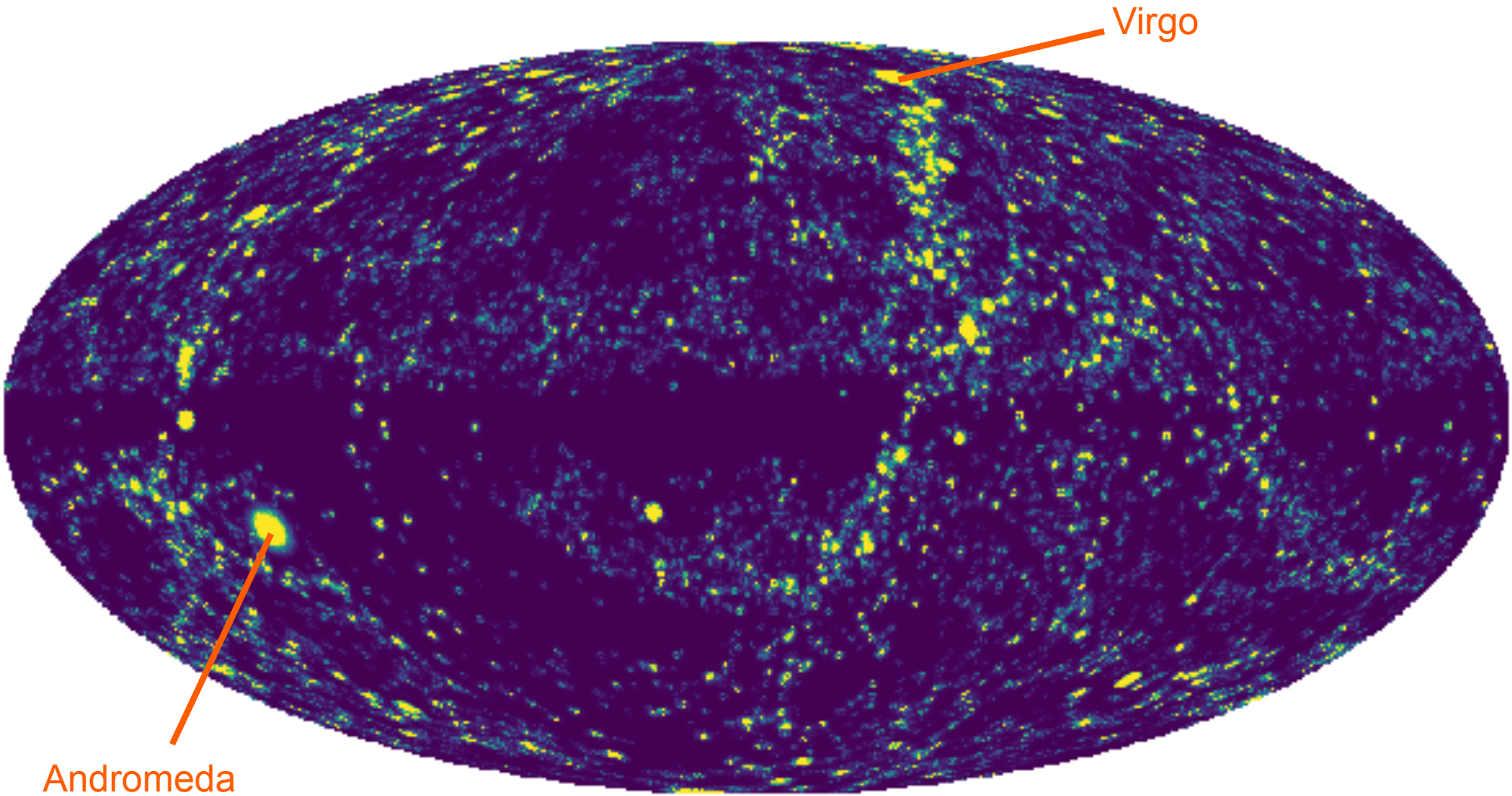


0 $\mathrm{GeV^2 cm^{-5}}$ 1e+16

$$J \sim (1 + \text{boost}) \int \rho^2_{\mathrm{NFW}}\, d\ell\, d\Omega$$

# Galaxy Group Limit

Lisanti, Mishra-Sharma, Rodd, Safdi, and Wechsler [1709.00416]
Lisanti, Mishra-Sharma, Rodd, and Safdi [1708.09385]

see parallel session talk by S. Mishra-Sharma (18:30)

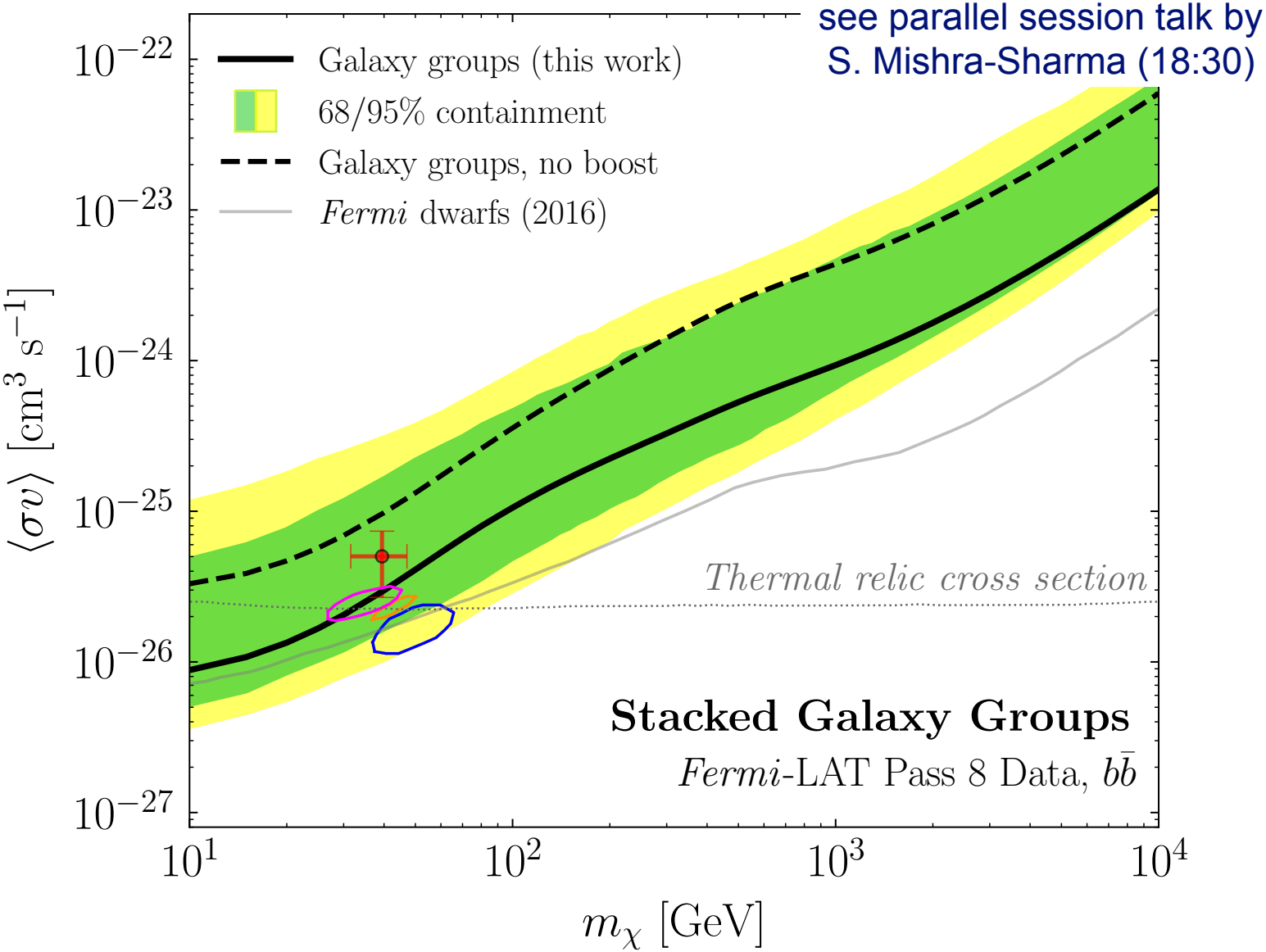

# Effect of Stacking

Order of magnitude gain in the limit achieved by stacking the galaxy groups

The brightest galaxy cluster does not dominate the bounds

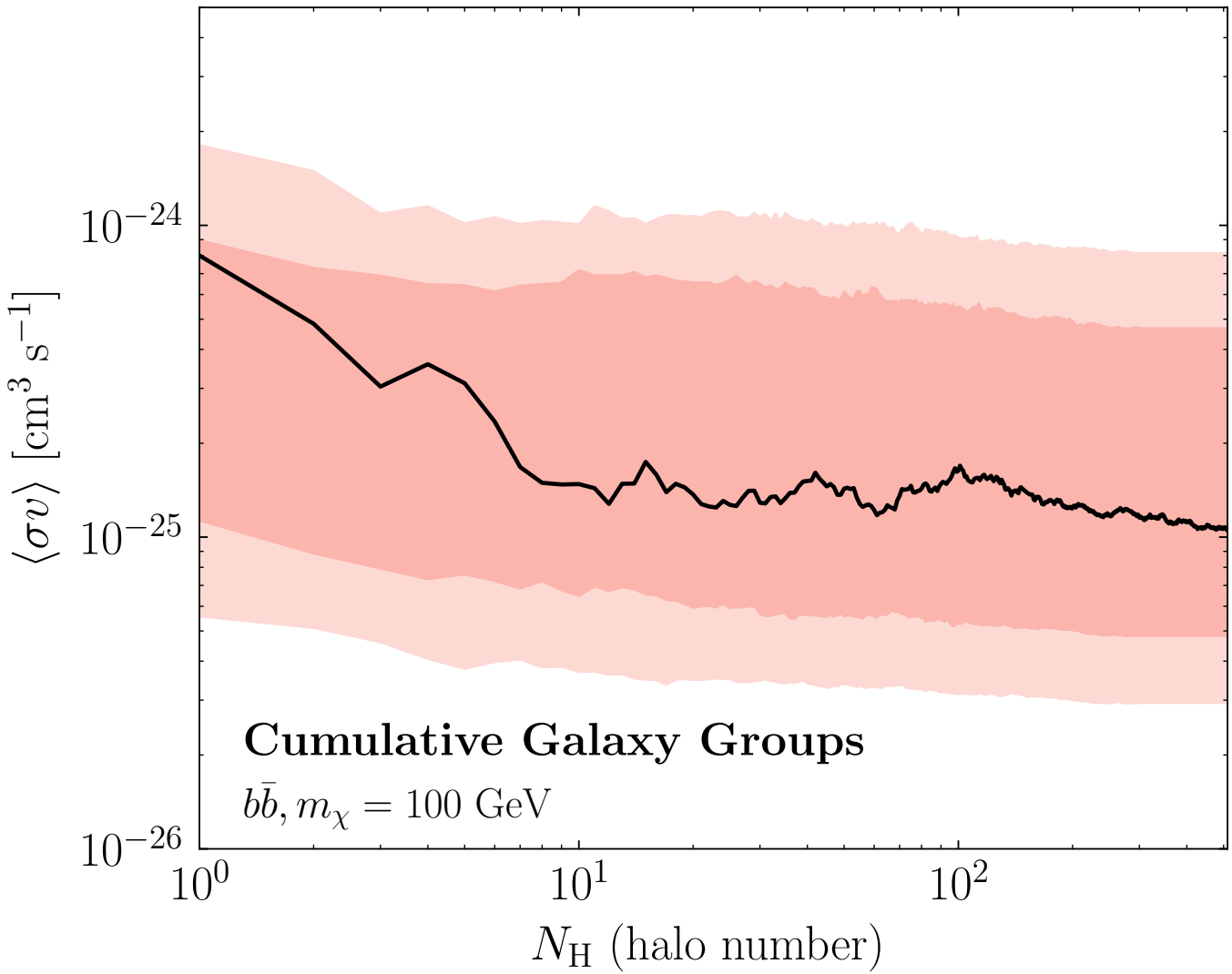

# Returning to the Milky Way...

What if we look for dark matter annihilation in the Milky Way halo, but away from the Galactic Center?

A comparison of the J-factors shows that the signal can still be brighter than that expected for dwarfs or galaxy groups

## J-factor Comparison

$$J = \int ds\, d\Omega\, \rho^2(s, \Omega)$$

| | |
|---|---|
| Dwarf Galaxy | ~$10^{19}$ GeV$^2$ cm$^{-5}$ sr |
| Brightest Groups | ~$10^{19}$ GeV$^2$ cm$^{-5}$ sr |
| Milky Way (20°x20°) | ~$10^{23}$ GeV$^2$ cm$^{-5}$ sr |
| Milky Way (ROI) | ~$10^{22}$ GeV$^2$ cm$^{-5}$ sr |

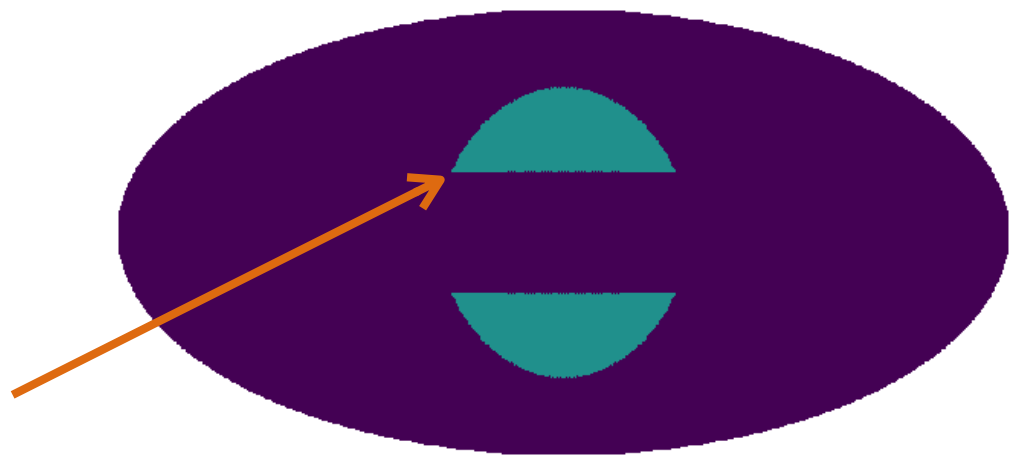

# Smooth Milky Way Halo

Chang, Lisanti, and Mishra-Sharma [1804.04132]

Excludes dark matter with mass below ~70 GeV that annihilates to b-quarks at the 95% confidence level—strongest limits in this range

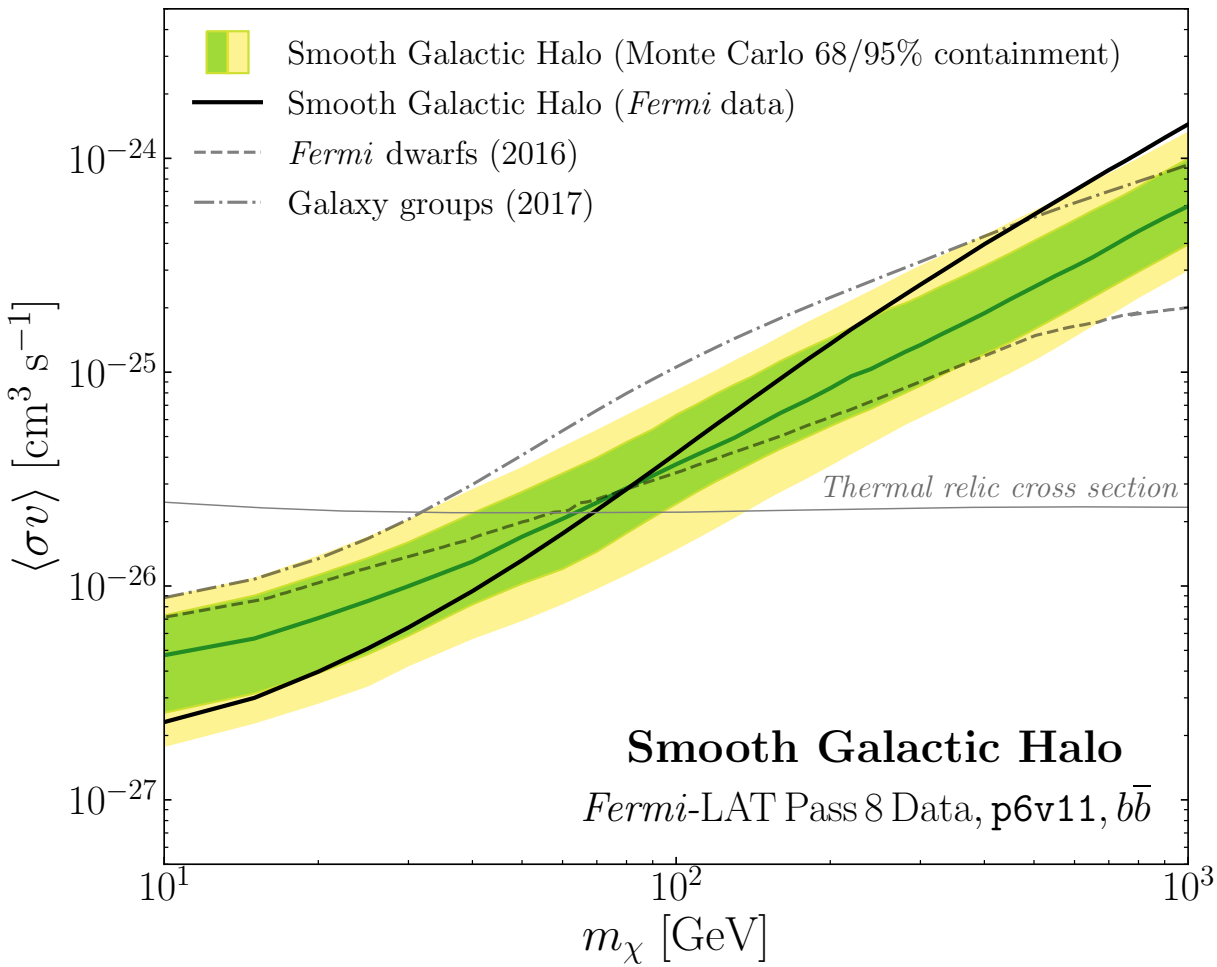

# Implications for GeV Excess

Chang, Lisanti, and Mishra-Sharma [1804.04132]

Excludes the b-channel interpretation of the GeV Excess and constrains the tau-channel for the first time

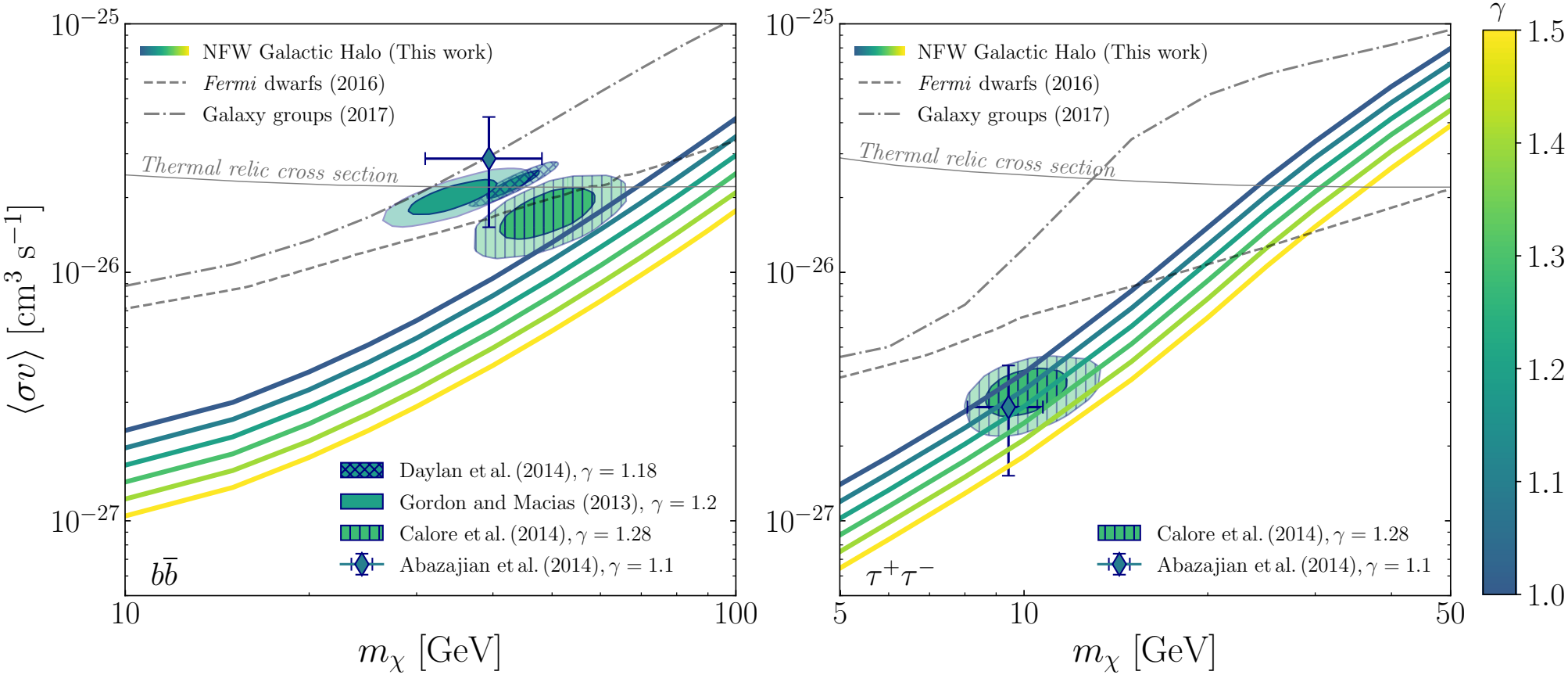


*See parallel session talk by S. Mishra-Sharma for complete discussion of foreground uncertainties*

# Conclusions

Abundance of evidence for an excess of GeV gamma-rays in the Galactic Center

Photon statistics and spatial morphology strongly suggest a stellar origin as opposed to emission from dark matter annihilation

Dark matter interpretation remains in tension with limits from dwarfs and groups

New search for annihilation in the Milky Way halo at high latitudes excludes the b-channel interpretation of the Excess, and puts the tau-channel interpretation in tension

# Back Up Slides

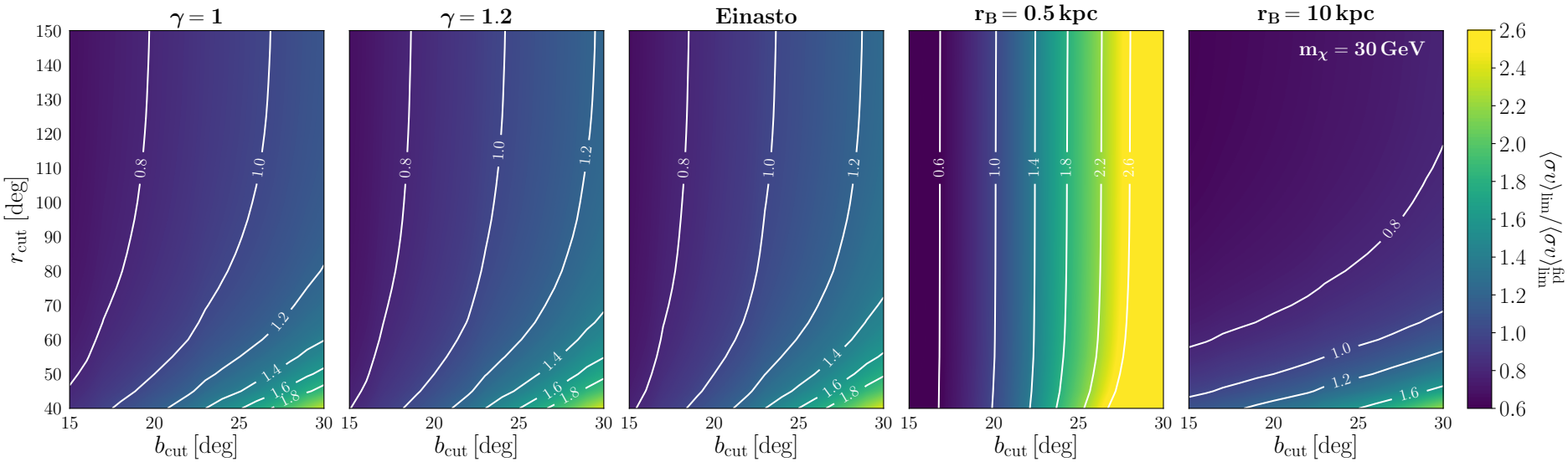


FIG. S1. Sensitivity projections for a 30 GeV dark matter particle annihilating to $b\bar{b}$ for different regions of interest, which are defined by latitude ($|b| > b_{\rm cut}$) and radial ($r < r_{\rm cut}$) cuts. The projected limit, $\langle\sigma v\rangle_{\rm lim}$, is compared to the limit for the fiducial region, $\langle\sigma v\rangle_{\rm lim}^{\rm fid}$, which corresponds to $|b| > 20^\circ$ and $r < 50^\circ$. The contours indicate the ratio of these two cross sections. The projections are provided for different dark matter density profiles: (left to right) generalized NFW with inner-slope $\gamma = 1, 1.2$, Einasto, and Burkert with a $r_B = 0.5$ and 10 kpc core.

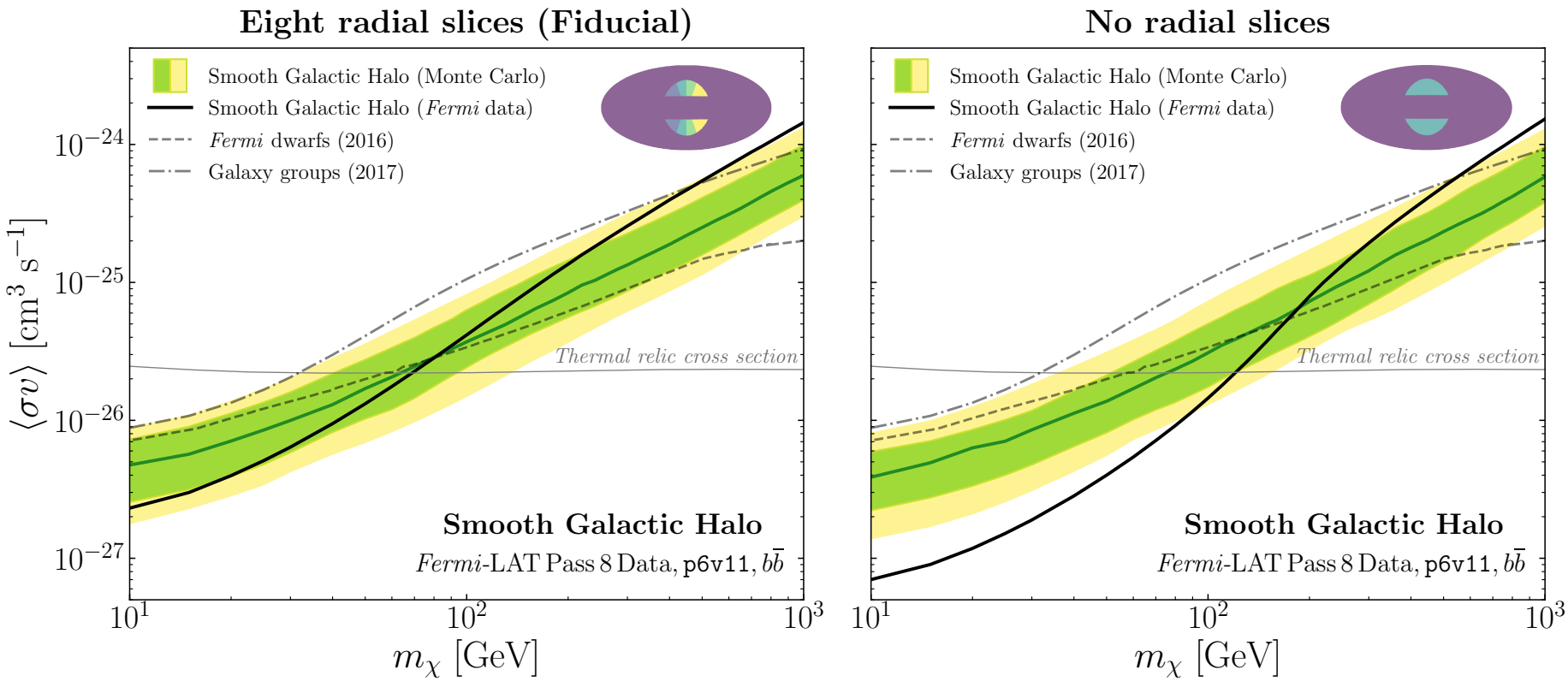


FIG. S2. (Left) Reproduction of Fig. 1 of the *Letter*, included here for convenience. (Right) The corresponding limits when the `p6v11` template is not divided into eight radial slices whose normalizations float independently in the fitting procedure. For each panel, the inset depicts the regions (not colored purple) over which the `p6v11` template is allowed to float.

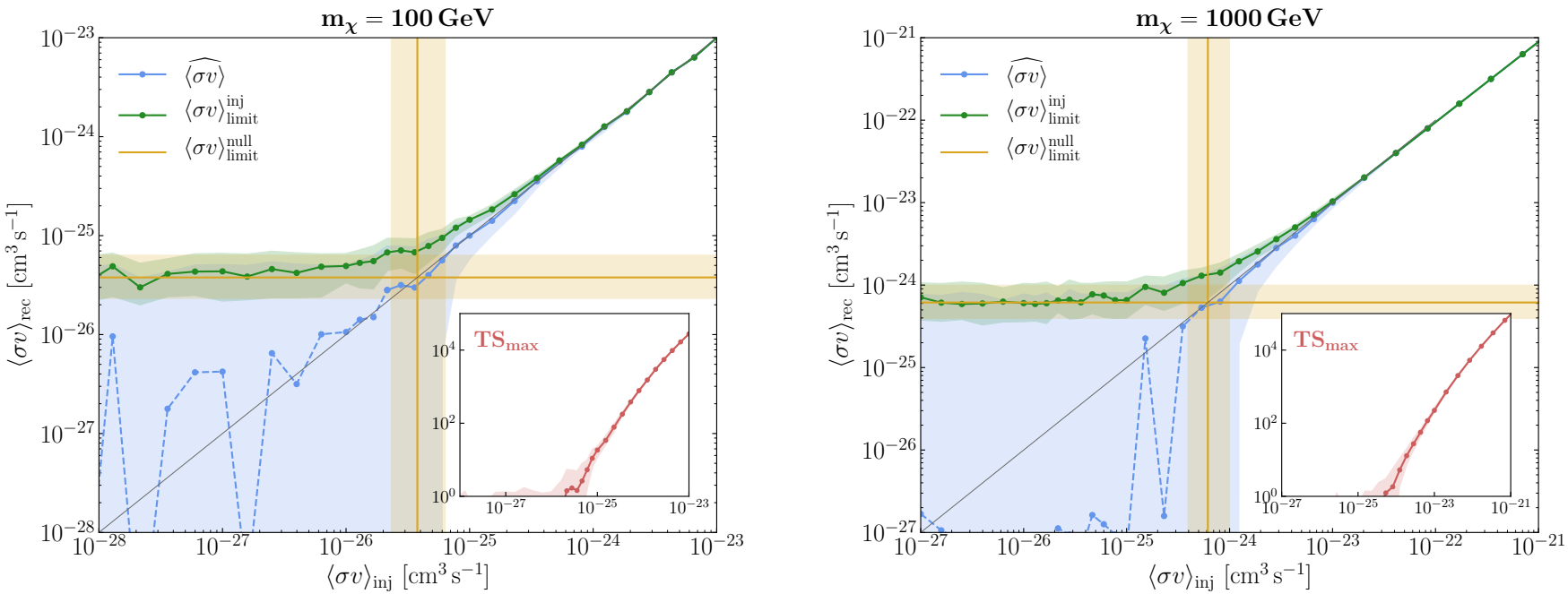


FIG. S3. Signal injection tests on Monte Carlo simulations for a 100 (left) and 1000 (right) GeV DM particle annihilating to $b\bar{b}$. In each panel, the gold line corresponds to the limit $\langle\sigma v\rangle^{\rm null}_{\rm limit}$ obtained when no signal is injected into the simulated data. The green line corresponds to the median cross section limit, $\langle\sigma v\rangle^{\rm inj}_{\rm limit}$, that is recovered for a given injected cross section $\langle\sigma v\rangle_{\rm inj}$, when TS $= -2.71$. The green band shows the corresponding 68% containment. The blue line corresponds to the median recovered cross section $\widehat{\langle\sigma v\rangle}$ that is associated with the maximum test statistic $\mathrm{TS_{max}}$ (plotted in the inset), and is shown as dashed in the regime where $\mathrm{TS_{max}} < 1$. The blue band spans extremal values of the 68% containment of cross sections associated with $\mathrm{TS_{max}} - 1$. For each injected signal point, we create 50 realizations of simulated sky maps.

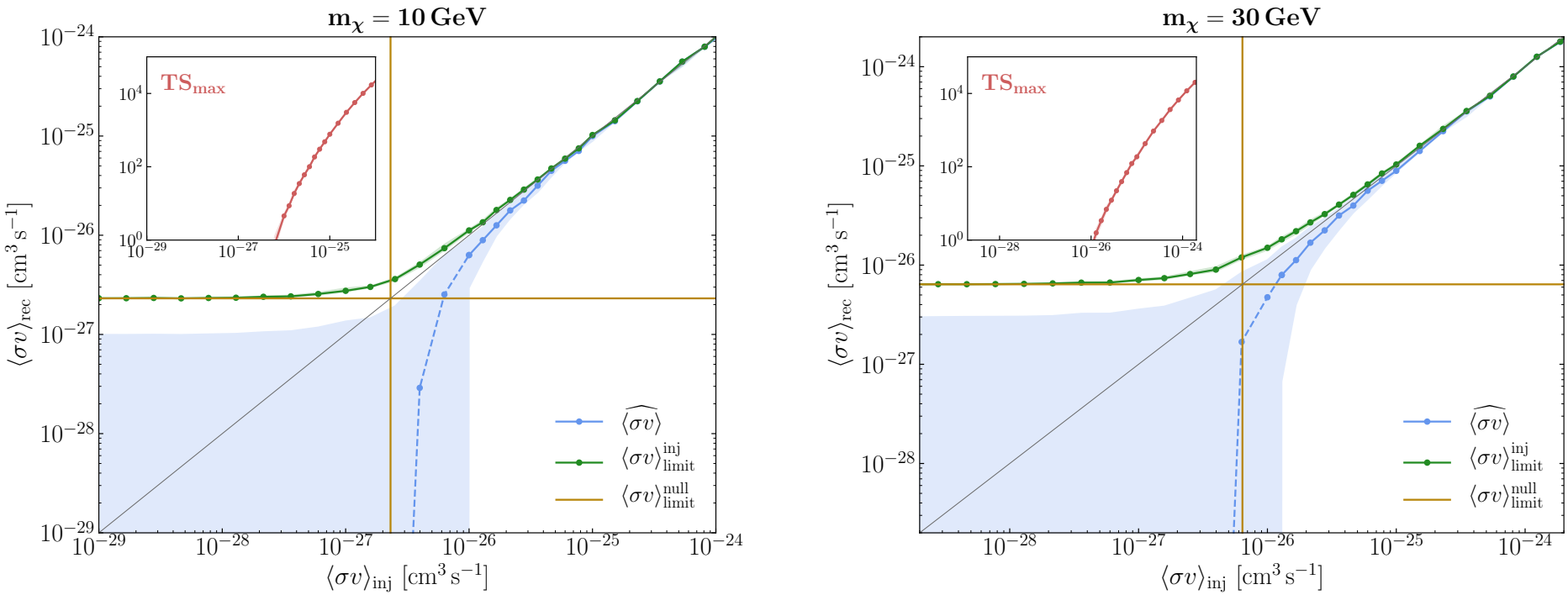


FIG. S4. The same as Fig. S3, except for signal injected on data. The left(right) panel corresponds to a 10(30) GeV DM mass. In this case, for each injected signal point, we create 10 realizations of simulated sky maps.

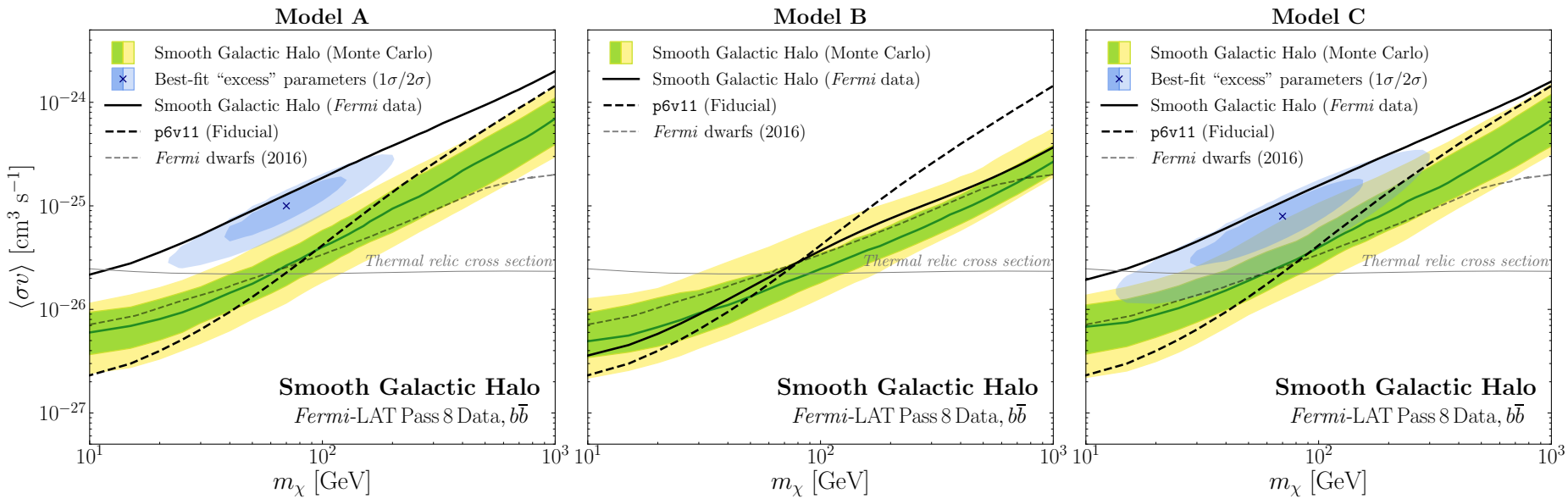


FIG. S5. Similar to Fig. 1 of the *Letter*, except using the Model A, B, and C foreground models (left, middle, and right panel, respectively) as provided by the *Fermi*-LAT Collaboration [8]. Note that the foreground templates are still divided into eight radial slices, as in the fiducial study, but the normalizations of the inverse-Compton and $\pi^0$+Bremsstrahlung templates are allowed to float independently. The fiducial limit obtained using the `p6v11` foreground model is shown by the dashed black line for comparison. The "excesses" in the Model A and C studies (with significances $\mathrm{TS}_{\mathrm{max}} \sim 28$ and 14, respectively) are well-understood in terms of the source populations included in these models; see text for further discussion. Model B is statistically preferred over Models A and C as a description of the data in our ROI; the difference in the maximum log-likelihood between Model B and A(C) is $\Delta \log \mathcal{L}_{\mathrm{max}} = 136(119)$.

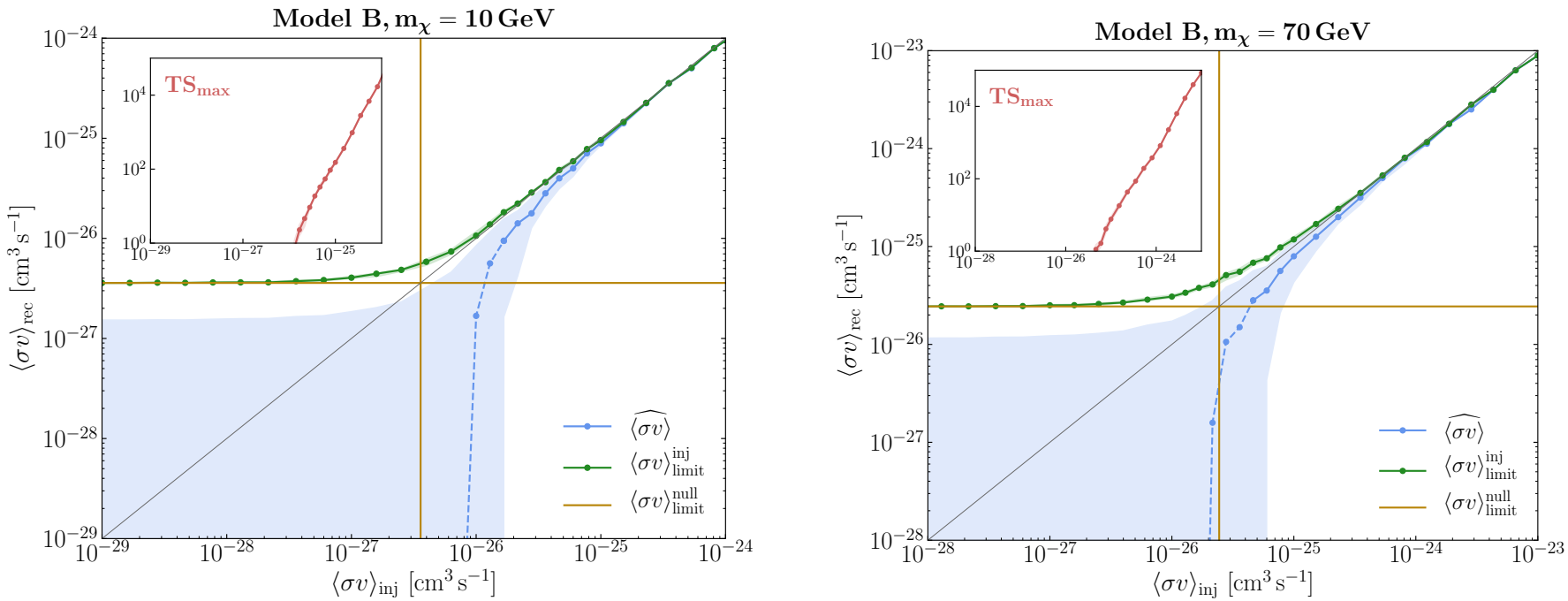


FIG. S6. Signal injection test on data using the Model B foreground template, assuming $m_\chi = 10$ GeV (left) and 70 GeV (right). Format as in Fig. S4.

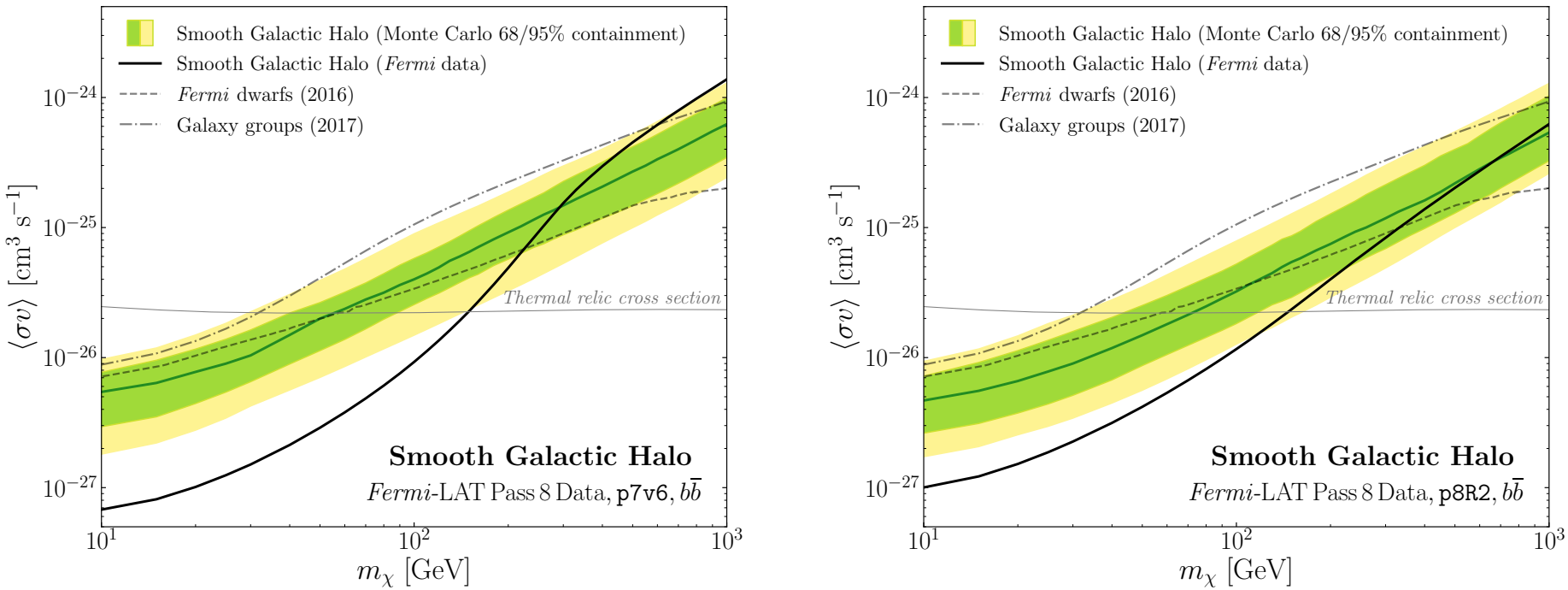


FIG. S7. Similar to Fig. 1 of the *Letter*, except using the `p7v6` and `p8R2` foreground models (left and right panel, respectively) [52]. We only include these results for illustration as both of these foreground models are not appropriate for studies of diffuse DM signals, as discussed in the text.

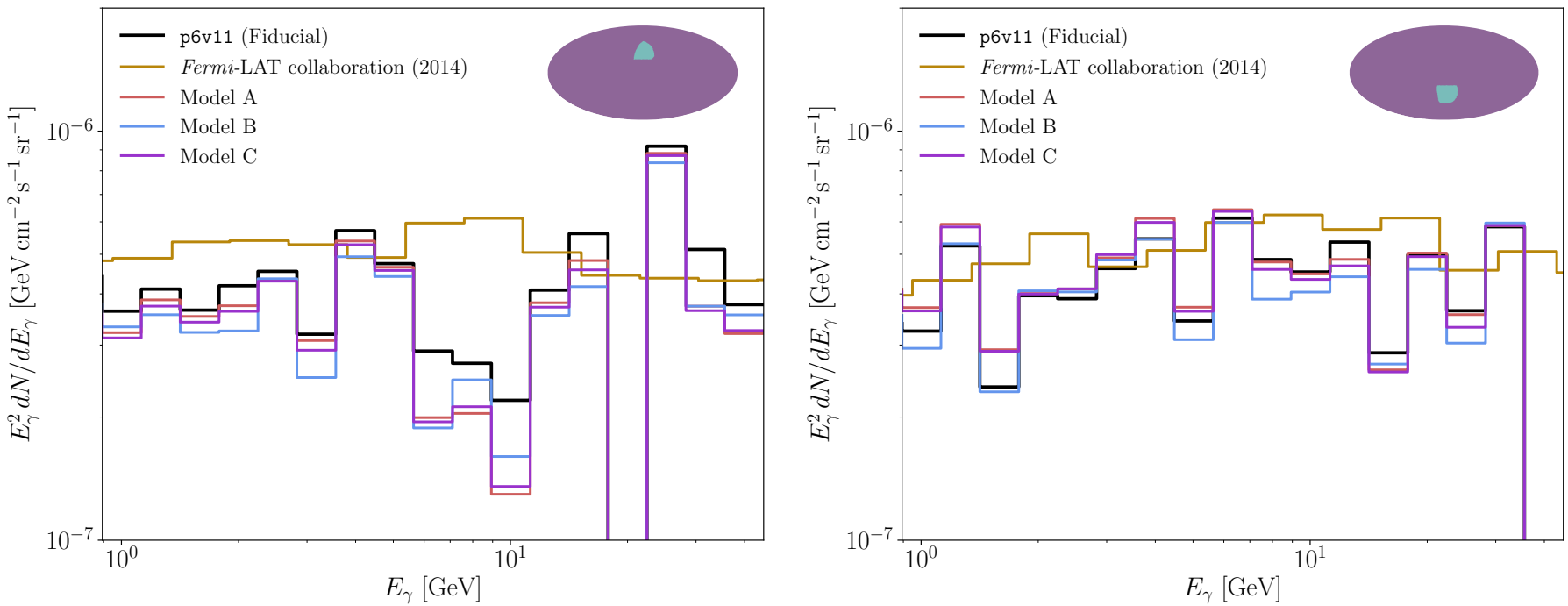


FIG. S8. Recovered spectra, normalized to the corresponding bubbles region shown, for the Northern (left) and Southern (right) lobes of the *Fermi* bubbles when analyzed with diffuse model `p6v11` as well as Models A, B and C. Our fiducial configuration was used to extract these spectra. The bubbles spectra obtained in [57] are shown for comparison. Note that a slighty different ROI ($|b| > 10^\circ$ as opposed to $|b| > 20^\circ$) was used in that case. The energy $E_\gamma$ corresponds to the geometric mean of the energy bin edges.

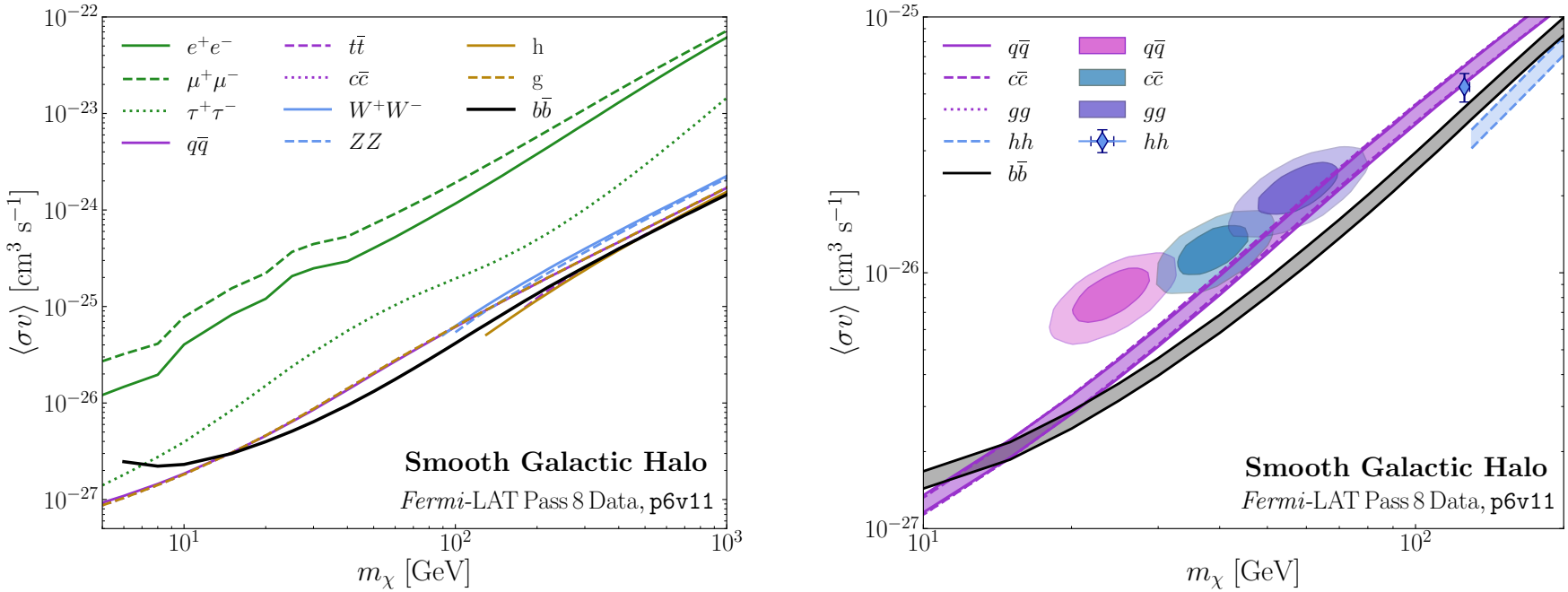


FIG. S9. (Left) The 95% confidence limit on dark matter of mass, $m_\chi$, annihilating with cross section, $\langle\sigma v\rangle$, in the smooth Galactic halo. The limits are obtained following the fiducial analysis procedure described in the *Letter*, but varying over the annihilation channel. (Right) The 95% confidence limits on dark matter annihilation into $b\bar{b}$ (fiducial), $q\bar{q}$, $c\bar{c}$, $gg$, and $hh$, varying over the inner slope, $\gamma$, of the generalized NFW density profile. The bands correspond to $\gamma$ values spanning 1.2–1.3. Note that the bands for $q\bar{q}$, $c\bar{c}$, and $gg$ fall essentially on top of each other. The best-fit parameters for the $q\bar{q}$, $c\bar{c}$, and $gg$ channels, as obtained in [75], are indicated by the pink, teal, and purple $1\sigma/2\sigma$ filled contours, respectively. The best-fit $hh$ value (and associated $1\sigma$ range) is indicated by the blue diamond [75].

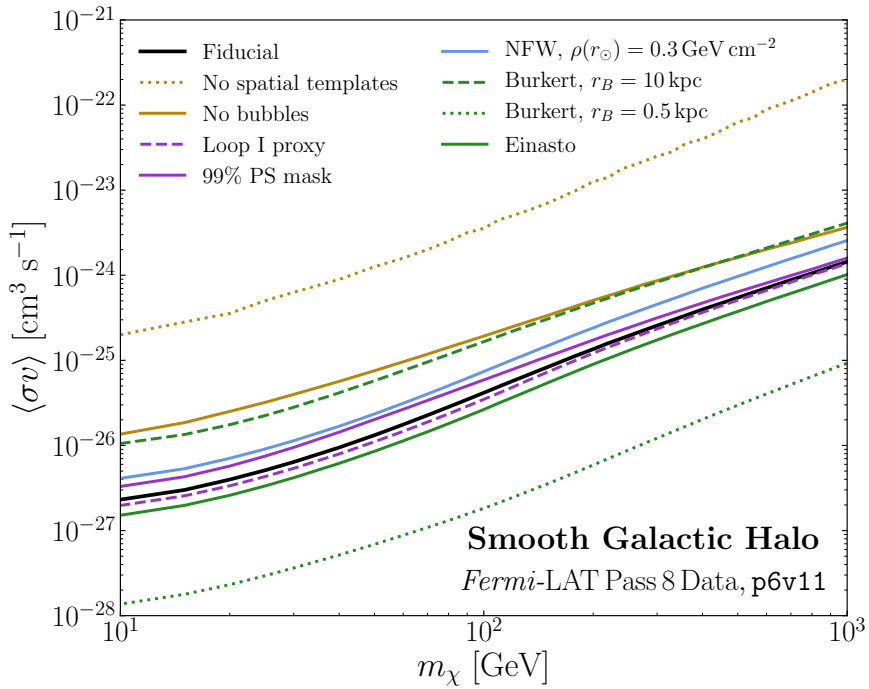


FIG. S10. The 95% confidence limits associated with variations to the fiducial analysis, as labeled in the legend and described in the text.